AD_____

Award Number: DAMD17-02-1-0506

TITLE: Nanoparticle-Mediated p53 Gene Therapy for Breast Cancer

PRINCIPAL INVESTIGATOR: Swayam Prabha
Vinod D. Labhasetwar, Ph.D.
Jamboor K. Vishwanathan

CONTRACTING ORGANIZATION: University of Nebraska Medical Center
Omaha, Nebraska 69198-7835

REPORT DATE: April 2003

TYPE OF REPORT: Annual Summary

PREPARED FOR: U.S. Army Medical Research and Materiel Command
Fort Detrick, Maryland 21702-5012

DISTRIBUTION STATEMENT: Approved for Public Release;
Distribution Unlimited

The views, opinions and/or findings contained in this report are
those of the author(s) and should not be construed as an official
Department of the Army position, policy or decision unless so
designated by other documentation.

20030701 130

REPORT DOCUMENTATION PAGE

Public reporting burden for this collection of information is estimated to average 1 hour per response, including the time for reviewing instructions, searching existing data sources, gathering and maintaining the data needed, and completing and reviewing this collection of information. Send comments regarding this burden estimate or any other aspect of this collection of information, including suggestions for reducing this burden to Washington Headquarters Services, Directorate for Information Operations and Reports, 1215 Jefferson Davis Highway, Suite 1204, Arlington, VA 22202-4302, and to the Office of Management and Budget, Paperwork Reduction Project (0704-0188), Washington, DC 20503

1. AGENCY USE ONLY (Leave blank)	2. REPORT DATE April 2003	3. REPORT TYPE AND DATES COVERED Annual Summary (15 Mar 02 - 14 Mar 03)

4. TITLE AND SUBTITLE
Nanoparticle-Mediated p53 Gene Therapy for Breast Cancer

5. FUNDING NUMBERS
DAMD17-02-1-0506

6. AUTHOR(S):
Swayam Prabha
Vinod D. Labhasetwar, Ph.D.
Jamboor K. Vishwanathan

7. PERFORMING ORGANIZATION NAME(S) AND ADDRESS(ES)

University of Nebraska Medical Center
Omaha, Nebraska 69198-7835

E-Mail: sprabha@unmc.edu

8. PERFORMING ORGANIZATION REPORT NUMBER

9. SPONSORING / MONITORING AGENCY NAME(S) AND ADDRESS(ES)

U.S. Army Medical Research and Materiel Command
Fort Detrick, Maryland 21702-5012

10. SPONSORING / MONITORING AGENCY REPORT NUMBER

11. SUPPLEMENTARY NOTES

12a. DISTRIBUTION / AVAILABILITY STATEMENT
Approved for Public Release; Distribution Unlimited

12b. DISTRIBUTION CODE

13. Abstract *(Maximum 200 Words)* *(abstract should contain no proprietary or confidential information)*

The effect of different formulation parameters on nanoparticle-mediated gene transfection *in vitro* was studied. Nanoparticles encapsulating plasmid DNA encoding fire fly luciferase were formulated using poly lactide (PLA) and poly dl-lactide *co*-glycolide (PLGA) polymers of different composition and molecular weight. A multiple emulsion solvent evaporation method with polyvinyl alcohol (PVA) as an emulsifier was used to formulate DNA-loaded nanoparticles. Transfection of various nanoparticles formulations was determined in breast cancer (MCF-7) cell line. Nanoparticles formulated with PLA demonstrated relatively lower transfection than those formulated with PLGA because of higher DNA release from PLGA nanoparticles than that from PLA nanoparticles. Further study demonstrated that the DNA loading in nanoparticles increases with increase in molecular weight of PLGA which results in enhanced gene expression. The nanoparticles surface-associated PVA was found to have significant effect on gene expression. Nanoparticles with higher amount of surface-associated PVA demonstrated reduced cellular uptake and also reduced the gene expression by 12 to 20 fold compared to the nanoparticles with lower amount of surface-associated PVA. The results of the study thus demonstrate that DNA loading in nanoparticles and its release rate as well as the surface-associated PVA influencing the interfacial properties of nanoparticles are some of the critical determinants in nanoparticle-mediated gene transfection.

14. SUBJECT TERMS:
sustained local gene delivery, apoptosis, nanoparticles, p53, polymer, non-viral gene delivery systems

15. NUMBER OF PAGES
39

16. PRICE CODE

17. SECURITY CLASSIFICATION OF REPORT Unclassified	18. SECURITY CLASSIFICATION OF THIS PAGE Unclassified	19. SECURITY CLASSIFICATION OF ABSTRACT Unclassified	20. LIMITATION OF ABSTRACT Unlimited

NSN 7540-01-280-5500

Table of Contents

INTRODUCTION

p53, a tumor suppressor gene, encodes a nuclear phosphoprotein involved in the control of cell growth and apoptosis. Breast cancer is associated with a high degree of mutations in the p53 gene that leads to loss of apoptotic control over cell proliferation. Transfection of tumor cells with p53 gene would result in the restoration of normal p53 protein functions in the cell. The purpose of this project is to investigate nanoparticles, a colloidal polymeric gene delivery system of ~100 nanometer diameter, formulated from a FDA-approved, biodegradable and biocompatible polymer, poly(DL-lactide-co-glycolide) (PLGA), for the treatment of breast cancer. Four specific aims proposed are as follows:

1. To formulate and characterize p53 gene-containing nanoparticles.
2. To study the mechanism of gene transfer using nanoparticles.
3. To study the sustained inhibition of proliferation of human breast cancer cells (MCF7) with p53 gene-loaded nanoparticles.
4. To study the efficacy of nanoparticle mediated p53 gene therapy in effecting a long-term tumor inhibition and regression in a mouse model of breast cancer.

This report summarizes the finding from the specific aim 1 and 2 and is outlined based on the statement of work.

Task 1: Formulation, months 1-12

1. Formulation and characterization of luciferase gene-loaded nanoparticles, months1-12.

Luciferase gene encoding DNA containing nanoparticles were formulated using different PLGA molecular weight (12 kDa, 53 kDa and 143 kDa) and composition (lactide: glycolide ratio 100:0 (PLA), 75:25 and 50:50), using solvent evaporation technique. Polyvinyl alcohol (PVA) is the commonly used surfactant in the formulation of the nanoparticles. In our previous studies(1), PVA was demonstrated to remain associated with the nanoparticles even after repeated washings and was found to affect the interfacial properties (Hydrophilicity and surface charge) and cellular uptake properties of the nanoparticles. Hence, various formulations of different surfactant type (degree of hydrolyzation: 80 % and 89 % and average molecular weight 13000-23000, 31000-50000 and 85000–146000) and concentration (0.5%, 2% and 5%) were also prepared. Nanoparticles were characterized for DNA loading, amount of PVA bound, size and zeta potential of the nanoparticles. Table 1-5 summarizes the effect of various formulation parameters on physical parameters of nanoparticles.

Table 1: Physical characterization of the nanoparticles formulated using PLGA of different molecular weight

PLGA Molecular Weight	PVA bound to nanoparticles (n=3)	Mean particle size (nm); (n=3)	Polydispersity Index (n=3)	Zeta potential (mV) ± S.E.M (n=3)	DNA loading (mg/100 mg nanoparticles)
12405	2.3 ± 0.9	563 ± 6	0.2 ± 0.02	-17.8 ± 1.0	1.8
53100	2.2 ± 0.3	685 ± 40	0.3 ± 0.02	-16.6 ± 1.4	1.7
143000	3.8 ± 0.4	375 ± 22	0.2 ± 0.01	-11.5 ± 3.4	2.9

Table 2: Physical characterization of the nanoparticles formulated using PLGA of different composition

PLGA Composition (lactide: glycolide ratio	PVA bound to nanoparticles (n=3)	Mean particle size (nm); (n=3)	Polydispersity Index (n=3)	Zeta potential (mV) ± S.E.M (n=3)	DNA loading (mg/100 mg nanoparticles)
100:0	2.4 ± 0.3	571 ± 9	0.2 ± 0.02	-14.3 ± 1.7	1.8
75:25	2.2 ± 0.2	485 ± 11	0.2 ± 0.01	-16.6 ± 1.4	1.9
50:50	2.2 ± 0.3	685 ± 40	0.3 ± 0.03	-18.2 ± 3.7	1.7

Table 3: Physical characterization of the nanoparticles formulated using PVA of different concentration

PVA concentration (%)	PVA bound to nanoparticles (n=3)	Mean particle size (nm); (n=3)	Polydispersity Index (n=3)	Zeta potential (mV) ± S.E.M (n=3)	DNA loading (mg/100 mg nanoparticles)
0.5	2.2 ± 0.2	693 ± 23	0.2 ± 0.04	-31.3 ± 1.6	1.1
2.0	3.8 ± 0.4	347 ± 3	0.2 ± 0.02	-11.5 ± 3.4	2.9
5.0	5.2 ± 0.7	270 ± 1	0.2 ± 0.01	-6.5 ± 1.7	2.9

Table 4: Physical characterization of the nanoparticles formulated using PVA of different molecular weight

PVA Molecular Weight (Da)	PVA bound to nanoparticles (n=3)	Mean particle size (nm); (n=3)	Polydispersity Index (n=3)	Zeta potential (mV) ± S.E.M (n=3)	DNA loading (mg/100 mg nanoparticles)
13000	5.7 ± 0.2	561 ± 22	0.1 ± 0.02	-15.62 ± 5.8	2.4
31000	4.1 ± 0.3	560 ± 2	0.2 ± 0.04	-17.28 ± 5.3	1.8
86000	3.7 ± 0.6	1207 ± 30	0.2 ± 0.04	-14.92 ± 4.7	1.9

Table 5: Physical characterization of the nanoparticles formulated using PVA of different degree of hydrolyzation

PVA Hydrolysis (%)	PVA bound to nanoparticles (n=3)	Mean particle size (nm); (n=3)	Polydispersity Index (n=3)	Zeta potential (mV) ± S.E.M (n=3)	DNA loading (mg/100 mg nanoparticles)
80	9.1 ± 0.9	344 ± 1	0.2 ± 0.01	-22.22 ± 1.8	1.3
89	5.7 ± 0.2	561 ± 22	0.1 ± 0.02	-15.62 ± 5.8	2.4

Conclusions

The conclusions for this task are that physical parameters are unaffected by the polymer composition, however polymer molecular weight and surfactant concentration are critical to formulate nanoparticle in suitable size range and with higher DNA loading. Low molecular weight and low surfactant concentration results in lower DNA loading in nanoparticles.

2. Study the effect of formulation parameters on DNA release kinetics, months 6-12.

In vitro DNA release was done as described in Prabha et al (2). The formulation parameters were found to affect the DNA release kinetics from the nanoparticles. Increasing the lactide content of the PLGA resulted in decrease in the amount of DNA released from the nanoparticles (Fig 1a). This could be because of slower diffusion of DNA from the highly hydrophobic polymer matrix. DNA release increases with increase in the PLGA molecular weight (Fig 1b). This is attributed to the higher DNA loading in the nanoparticles formulated from high molecular weight PLGA (Table 2). Increase in the PVA concentration resulted in increase in the DNA release with almost similar release from the nanoparticles using PVA concentration of 2 % and 5 % (Fig 3a). PVA molecular weight was not found to affect the DNA release (Fig 3b) despite differences in the DNA loading (Table 4). DNA release increases with the increase in the degree of hydrolyzation
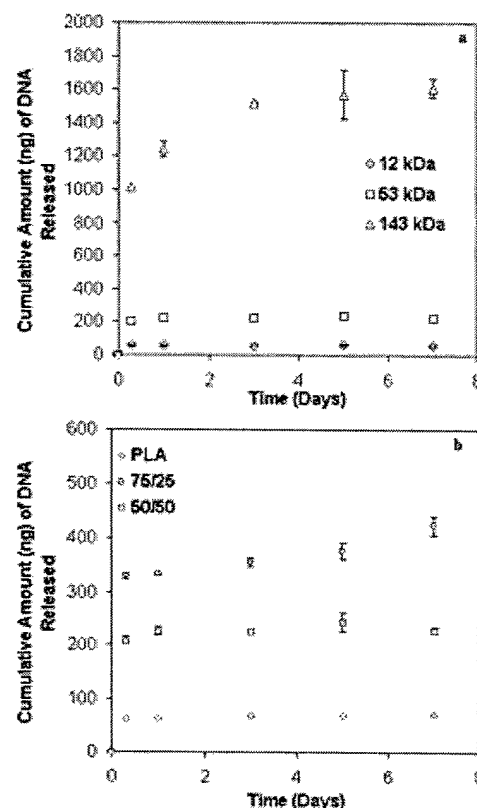

Fig 1 Effect of polymer molecular weight (a) and composition (b) on in vitro DNA release from nanoparticles
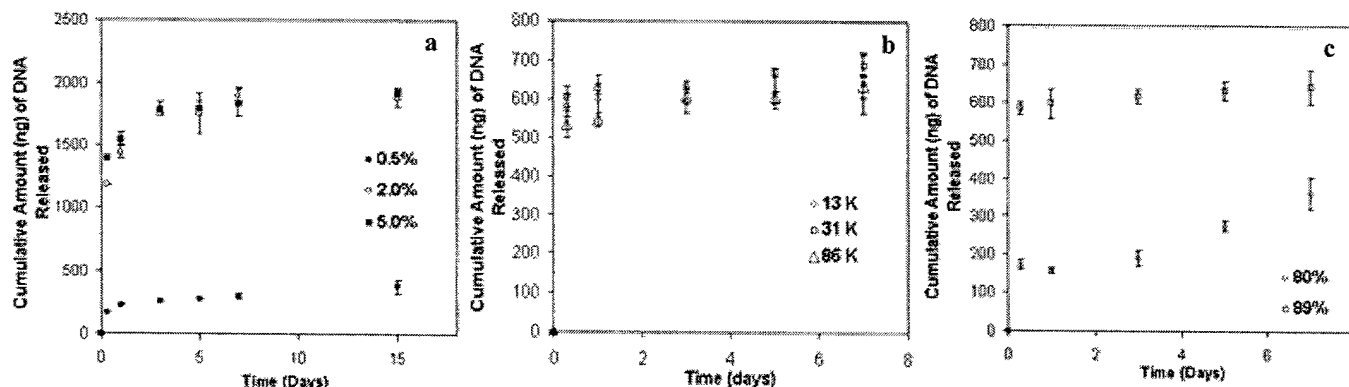

Fig 2: Effect of PVA concentration (a) PVA molecular weight (b) and PVA degree of hydrolyzation (c) on in vitro DNA release from nanoparticles (Data represented as mean ± SEM)

5

of PVA (Fig 3c). This can be explained based on the increased hydration of nanoparticle surface with the increase in the degree of hydrolyzation of PVA molecules associated with the nanoparticle surface that could lead to higher diffusion of DNA following rapid hydrolytic degradation of polymer matrix (3).

Task 2: Cell culture studies, months 6-18 (ongoing)

1. <u>Study the effect of various formulation parameters on the *in vitro* transfection efficiency of nanoparticles in cell culture, months 6-12.</u>

Transfection efficiency of nanoparticle was found to increase with decrease in the lactide content of the polymer (Fig 3a) and increase in PLGA molecular weight (Fig 3b) Nanoparticles formulated using PLA showed very low transfection efficiency which could be due to the decreased amount of DNA releases for similar amount of the nanoparticles. There were no significant differences (p > 0.05) between nanoparticles formulated using PLGA containing either 50 % or 75 % glycolide (Fig 5). This is attributed to the similar DNA loading in the two nanoparticle
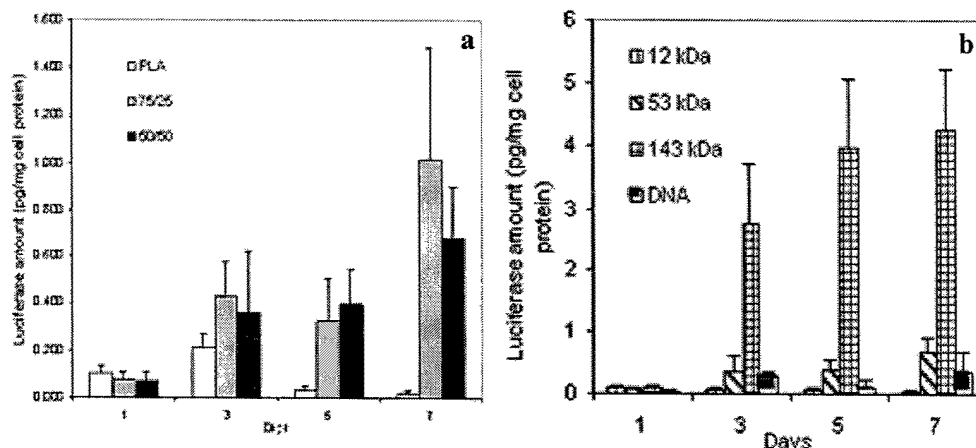

Figure 3: Effect of polymer composition (a) and polymer molecular weight (b) on nanoparticle-mediated gene expression in MCF-7. 75/25 and 50/50 represents lactide: glycolide ratio in PLGA (Data as mean ± SEM, n=6).

formulation. Nanoparticle-mediated gene transfection increases with the increase in PLGA molecular weight due to the increase in DNA loading and hence DNA release from nanoparticles formulated using higher molecular weight nanoparticles. Nanoparticles formulated using PLGA of molecular weight 143 kDa showed sustained gene transfection for up to seven days after which the studies could not be conducted in cell culture model.

PVA concentration and type was also found to affect the gene transfection properties of the nanoparticles. Gene transfection decreases with increase in the concentration of the PVA. This could be due to the higher amount of PVA associated with the nanoparticles formulated using higher concentration of the PVA. Despite lower DNA loading, nanoparticles prepared using 0.5 % PVA showed higher transfection compared to 5 % PVA nanoparticles. There were 12-20 fold differences in the transfection levels of nanoparticles formulated using 2 % and 5 % PVA (Fig 4a). Despite similar DNA release, gene transfection increases with increase in
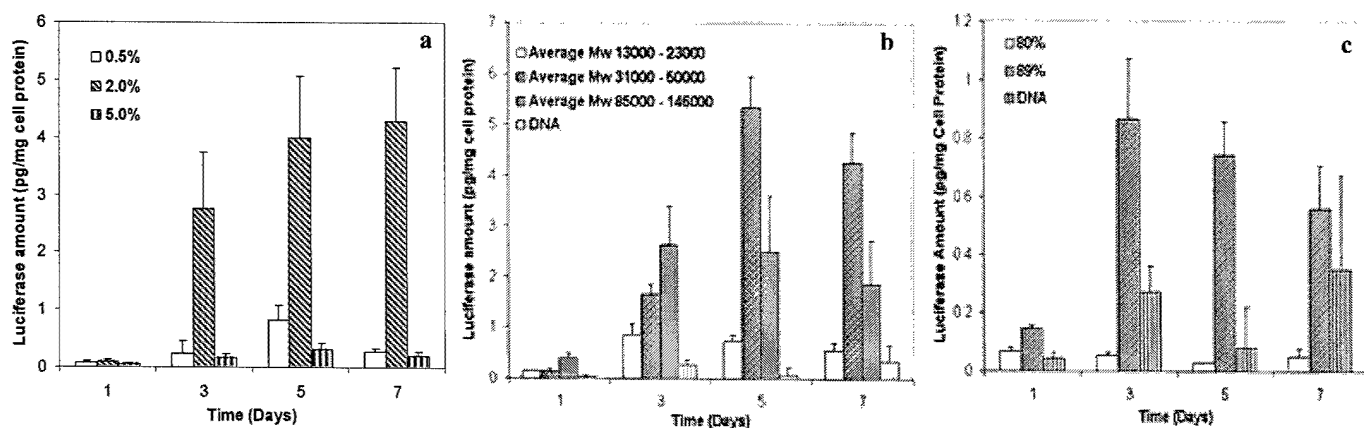

Fig 4: Effect of PVA concentration (a), molecular weight (b) and degree of hydrolyzation (c) on transfection efficiency of nanoparticles (Data represented as mean ± SEM). Naked DNA was used as a control.

PVA molecular weight that levels off beyond PVA of molecular weight 30,000-50,000 (Fig 4b). The higher amount of PVA associated with the nanoparticles formulated using PVA of low molecular weight could be the

reason for their low transfection. Degree of hydrolyzation of PVA was also found to affect the gene transfection. Transfection increases with the increase in the degree of hydrolyzation of the PVA (Fig 4c). This was due to the increase in the DNA release with the increase in the degree of hydrolyzation of PVA (Fig 4c). The studies suggest the role of interfacial properties on the gene transfection of nanoparticles.

2. <u>Investigate the cellular uptake and intracellular disposition characteristics of nanoparticles by chromatographic techniques, months 9-12.</u>

Effect of various formulation parameters on cellular uptake and intracellular distribution were studied in order to correlate the differences in transfection levels of different formulations and to investigate the mechanism of nanoparticle-mediated gene transfection. We have proposed the mechanism of intracellular trafficking of the nanoparticles (4). The findings of our studies suggest that intracellular uptake, retention, endosomal escape and DNA release are the important parameter governing the nanoparticle-mediated gene transfection.

Fig 5 represents the effect of polymer composition on the cellular uptake and retention of nanoparticles. It was found that nanoparticles formulated using polymer containing higher lactide amount resulted in the overall lower intracellular uptake of the nanoparticles. The results from the DNA release and uptake studies suggested that the nanoparticles formulated using higher polymer with higher lactide content are not suitable for the transfection as it results not only in the lower amount of nanoparticles inside the cells but also lower DNA available for transfection.

Fig 5: Effect of polymer composition on cellular uptake of nanoparticles

Fig 6 represents the intracellular uptake of nanoparticles formulated using different concentration of PVA. There were no significant difference in the uptake of the nanoparticles formulated using 0.5 % and 2 % PVA. However there was 1.5 fold reduced uptake of nanoparticles formulated using 5 % of PVA. Further the retention of the nanoparticles prepared using 5 % PVA was almost 2-fold lower than the nanoparticles prepared using lower concentration of PVA. Further intracellular distribution studies carried using a standard cell fractionation protocol (BioVision, CA) demonstrated two fold higher cytoplasmic levels of nanoparticles formulated using 2 % and 0.5 % of PVA compared to that prepared using 5% PVA (Fig 7). The studies indicate better endosomal escape of the nanoparticles formulated using lower concentration of PVA.

Overall findings from this task are that the nanoparticle mediated gene transfection is affected by the cellular uptake, retention and the endosomal escape of the nanoparticles. The nanoparticles demonstrating higher DNA loading and release also demonstrated higher cellular uptake and better endosomal escape. Future studies would be to investigate the mechanism of better endosomal escape.

Fig 6: Effect of PVA concentration on cellular uptake of nanoparticles
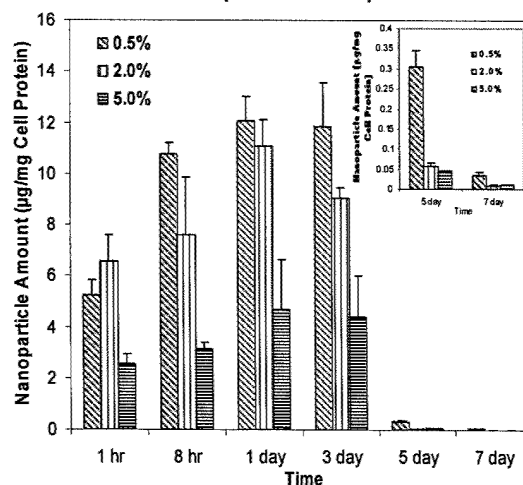
Fig 7: Effect of PVA concentration on cytoplasmic levels of nanoparticles

3. <u>Optimization of formulation parameters, months 2-8</u>

From the results of this specific aim, nanoparticles of PLGA of molecular weight 143 kDa and composition 50:50 formulated using 2 % external PVA were found to be best for
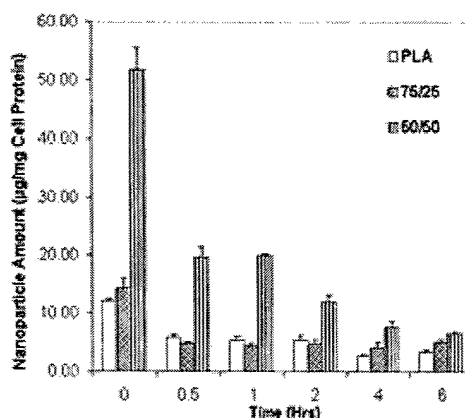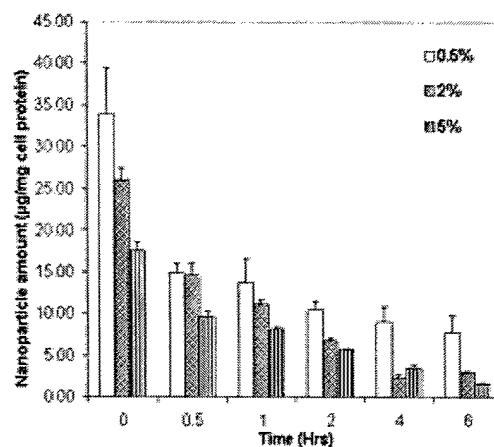
7

the gene transfection and will be used to formulate p53 loaded nanoparticles to study effect of p53 on cell cycle arrest and in vivo gene delivery.

Key Research accomplishments during last year
1. Parameters were optimized to increase the DNA loading and DNA release from the nanoparticles. This was useful in enhancing the transfection.
   - PLGA of molecular weight 143 kDa and composition 50:50 was found to be suitable in terms of DNA loading, DNA release and sustained gene transfection.
   - Interfacial properties of nanoparticles were found to affect their gene transfection. PVA of molecular weight 30,000-50000 and degree of hydrolyzation 89% used at the concentration of 2 % was found to be suitable in terms of particle size, DNA loading, DNA release and gene transfection.
2. Gene transfection was correlated to the cellular uptake and retention and endolysosomal escape of nanoparticles that provided the insight in the mechanism of gene transfection in part.

Reportable outcomes
1. PLGA composition was found to have no effect on any of physical properties of nanoparticles. Gene transfection decreases with the increase in the lactide content of the nanoparticles. Lower DNA release from the hydrophobic matrix and lower cellular uptake were found to be the parameters affecting the gene transfection.
2. Increase in PLGA molecular weight was associated with the increase in the DNA loading of the nanoparticles. Gene transfection also increases with the increase in the PLGA molecular weight. Higher DNA loading and DNA release were found to be the factors responsible for higher gene transfection.
3. Nanoparticles showed sustained gene transfection for up to seven days in cell culture model.
4. Interfacial properties of nanoparticles that in turn was affected by the surfactant used in the formulation of the nanoparticles, was found to influence the gene transfection. Increase in the PVA associated to the nanoparticles was associated with the decreased intracellular uptake and cytoplasmic levels of nanoparticles that resulted in lower gene transfection with the nanoparticles containing higher amount of the PVA.

Conclusions
In conclusion, various formulation factors and the interfacial properties of nanoparticles play an important role in the nanoparticle-mediated gene transfection. DNA loading and its release are important factors in enhancing gene expression using nanoparticles. The results of the study would be helpful in formulating the nanoparticles with p53 gene that would be used for in vivo tumor inhibition.

References
1. Sahoo, S. K., Panyam, J., Prabha, S., and Labhasetwar, V. (2002) Residual polyvinyl alcohol associated with poly (D,L-lactide-co-glycolide) nanoparticles affects their physical properties and cellular uptake. *J Control Release* 82, 105-114
2. Prabha, S., Zhou, W. Z., Panyam, J., and Labhasetwar, V. (2002) Size-dependency of nanoparticle-mediated gene transfection: studies with fractionated nanoparticles. *Int J Pharm* 244, 105-115
3. Murakami, H., Kawashima, Y., Niwa, T., Hino, T., Takeuchi, H., and Kobayashi, M. (1997) Influence of degree of hydrolyzation and polymerization of polyvinyl alcohol on the preparation and properties of poly (DL-lactide-co-glycolide) nanoparticle. *Int J Pharm* 149, 43 - 49
4. Panyam, J., Zhou, W. Z., Prabha, S., Sahoo, S. K., and Labhasetwar, V. (2002) Rapid endo-lysosomal escape of poly (DL-lactide-co-glycolide) nanoparticles: implications for drug and gene delivery. *Faseb J* 16, 1217-1226

Size-dependency of nanoparticle-mediated gene transfection: studies with fractionated nanoparticles

Swayam Prabha [a], Wen-Zhong Zhou [a], Jayanth Panyam [a], Vinod Labhasetwar [a,b,*]

[a] *Department of Pharmaceutical Sciences, 986025 University of Nebraska Medical Center, Omaha, NE 68198-6025, USA*
[b] *Department of Biochemistry, University of Nebraska Medical Center, Omaha, NE 68198-4525, USA*

Abstract

Nanoparticles formulated from biodegradable polymers such as poly (lactic acid) and poly (D,L-lactide-co-glycolide) (PLGA) are being extensively investigated as non-viral gene delivery systems due to their sustained release characteristics and biocompatibility. PLGA nanoparticles for DNA delivery are mainly formulated using an emulsion-solvent evaporation technique. However, this formulation procedure results in the formation of particles with heterogeneous size distribution. The objective of the present study was to determine the relative transfectivity of the smaller- and the larger-sized fractions of nanoparticles in cell culture. PLGA nanoparticles containing a plasmid DNA encoding luciferase protein as a marker were formulated by a multiple emulsion-solvent evaporation method (mean particle diameter $= 97 \pm 3$ nm) and were fractionated using a membrane (pore size: 100 nm) filtration technique. The particles that passed through the membrane were designated as the smaller-sized nanoparticles (mean diameter $= 70 \pm 2$ nm) and the fraction that was retained on the membrane as the larger-sized nanoparticles (mean diameter $= 202 \pm 9$ nm). The smaller-sized nanoparticles showed a 27-fold higher transfection than the larger-sized nanoparticles in COS-7 cell line and a 4-fold higher transfection in HEK-293 cell line. The surface charge (zeta potential), cellular uptake, and the DNA release were almost similar for the two fractions of nanoparticles, suggesting that some other yet unknown factor(s) is responsible for the observed differences in the transfection levels. The results suggest that the particle size is an important factor, and that the smaller-sized fraction of the nanoparticle formulation predominantly contributes towards their transfection. © 2002 Elsevier Science B.V. All rights reserved.

Keywords: Non-viral vectors; Gene therapy; Biodegradable polymers; Cellular uptake

1. Introduction

Gene therapy, the introduction of an extraneous gene into a cell with the aim of replacing a lost cellular function or to introduce a new func-

* Corresponding author. Tel.: + 1-402-559-9021; fax: + 1-402-559-9543
E-mail address: vlabhase@unmc.edu (V. Labhasetwar).

tionality, is fast becoming a reality (Rubanyi, 2001). However, achieving an efficient gene delivery into the target cell population or tissue without causing any vector-associated toxicity is critical to the success of gene therapy (Clark and Johnson, 2001). To achieve the above objective, various viral and non-viral vectors have been investigated (Kataoka and Harashima, 2001). Although viral vectors such as adenovirus, influenza virus and adeno-associated virus (Kochanek et al., 2001) are relatively more efficient in gene transfection than non-viral methods (Li and Huang, 2000), their toxicity and immunogenicity are the major concerns. Therefore, non-viral vectors such as liposomes, cationic block copolymers, polymer complexes, and micro- and nanoparticles have gained importance because they are relatively safe and are easy to formulate (Luo et al., 1999; Maheshwari et al., 2000). More recently, biodegradable nanoparticles formulated using different polymers such as chitosan (Mao et al., 2001; Roy et al., 1999), gelatin (Truong-Le et al., 1998), and other biodegradable polymers (Roy et al., 1999; Cohen et al., 2000) are being investigated as non-viral gene delivery systems because of the possibility of achieving safe and sustained gene transfection.

We have been investigating biodegradable nanoparticles formulated from poly (D,L-lactide-co-glycolide) (PLGA), an FDA approved biocompatible and biodegradable polymer, as a non-viral gene delivery system (Labhasetwar et al., 1999). Nanoparticles, because of their subcellular size, are effectively endocytosed by the cells which could result in higher cellular uptake of the entrapped DNA (Panyam et al., 2002b; Davda and Labhasetwar, 2002). Recently, we have demonstrated the rapid escape of PLGA nanoparticles from the endo-lysosomal compartment into cytoplasm, suggesting the suitability of nanoparticles as a gene delivery vector (Panyam et al., 2002b). Since the DNA is encapsulated inside the polymeric matrix, it would be protected from extracellular and intracellular nuclease degradation (Hedley et al., 1998). The DNA entrapped in nanoparticles is released slowly with the hydrolysis of the polymer matrix

due to the cleavage of the ester bonds. It is hypothesized that the slow release of DNA from nanoparticles intracellularly would be effective in achieving sustained gene expression in the target tissue. Sustained and regulated gene expression is probably more important in treating certain localized disease conditions such as the cardiac and limb ischemia by inducing neovascularization in the damaged tissue using genes encoding pro-angiogenic growth factors (Richardson et al., 2001). Similarly, sustained gene expression has been shown to be effective in bone regeneration, which could be useful to repair fractured bones (Bonadio et al., 1999). Restenosis, a vasculoproliferative condition that occurs following coronary balloon angioplasty procedure, is another example of a pathological condition where sustained gene expression in the target artery could be more effective (Ohno et al., 1994; Klugherz et al., 2000).

Various formulation factors and characteristics of nanoparticles could influence the transfectivity of nanoparticles. One of the important parameters that could affect the transfectivity of nanoparticles is their size. The particle size has been an important consideration while formulating other particulate type systems such as DNA-polymer (Dauty et al., 2001) and lipid complexes (Lee et al., 2001) and liposomes (Sakurai et al., 2000). Our studies and that of others have shown that the particle size significantly affects their cellular and tissue uptake (Desai et al., 1997; Zauner et al., 2001), and in some cell lines, only the submicron size particles are taken up efficiently but not the larger size microparticles (e.g. Hepa 1-6, HepG2, and KLN 205) (Zauner et al., 2001). Nanoparticles prepared by emulsion-solvent evaporation technique using PLGA polymer usually results in the formation of nanoparticles with heterogeneous particle size distribution. We hypothesized that the transfectivity of the different sized nanoparticle fractions in the formulation could be different. Therefore, the objective of the present study was to determine the relative transfectivity of the smaller- and the larger-sized fractions of nanoparticles in cell culture.

2. Materials and methods

2.1. Materials

PLGA (MW 143 900 Da, copolymer ratio 50:50) was purchased from Birmingham Polymers, Inc. (Birmingham, AL). Acetylated bovine serum albumin (Ac-BSA), MEM non-essential amino acid solution (100 ×), and polyvinyl alcohol (PVA, average MW 30 000–70 000) were purchased from Sigma Chemical Co. (St. Louis, MO). Fetal bovine serum (FBS, heat inactivated), 1 × trypsin-EDTA, Dulbecco's modified essential medium (DMEM), and penicillin-streptomycin were obtained from Gibco-BRL (Grand Island, NY). African green monkey kidney epithelial (COS-7) and human embryonic kidney epithelial (HEK-293) cells were purchased from American Type Culture Collection (ATCC) (Manassas, VA). Luciferase plasmid with simian virus 40 (SV40) promoter (pGL3), DNA molecular weight markers, cell culture lysis reagent (CCLR, 5 ×), luciferase assay kit, and the recombinant luciferase protein were purchased from Promega (Madison, WI). 6-Coumarin was purchased from Polyscience Inc. (Warrington, PA).

2.2. Methods

2.2.1. Formulation of nanoparticles containing plasmid DNA

Plasmid pGL3 containing firefly luciferase gene under the control of SV40 promoter was used as a marker DNA to study the transfectivity of nanoparticles. The DNA-loaded nanoparticles were formulated by a double emulsion-solvent evaporation technique (Labhasetwar et al., 1999). In brief, an aqueous solution containing 1 mg of DNA and 2 mg of Ac-BSA in 200 μl of Tris–EDTA (TE) buffer (pH 8.0) was emulsified into 1 ml of polymer solution in chloroform (30 mg PLGA/ml) using a probe sonicator (XL 2015 sonicator® ultrasonic processor, Misonix Inc., Farmingdale, NY) at 55 W of energy output for 1 min over an ice bath. The primary emulsion was then emulsified into 6 ml of 2% w/v aqueous solution of PVA using sonication as above for 5 min to form a multiple (water-in-oil-in-water)

emulsion. The emulsion was stirred at room temperature for ~18 h to evaporate chloroform. Nanoparticles thus formed were recovered by ultracentrifugation at 35 000 rpm (Beckman Optima™ LE-80K, Beckman Instruments, Inc., Palo Alto, CA), washed three times with distilled water to remove PVA and unentrapped DNA, resuspended in water, and lyophilized for 48 h (VirTis Co., Inc. Freeze Dryer, Gardiner, NY). All the washings following the recovery of nanoparticles were saved to determine the total DNA that was not encapsulated into nanoparticles (see Section 2.2.5 for DNA loading).

2.2.2. Fractionation of nanoparticles into different sizes

Lyophilized nanoparticles were resuspended in 10 ml of water by sonication for 2 min as above. Nanoparticles were then fractionated into two sizes by passing the suspension through a Durapore® VVPP membrane of porosity cut off 100 nm (Millipore, Bedford, MA) using an Amicon® membrane filtration system (Millipore). Fractionation of nanoparticles was carried out at a nitrogen pressure of 50 psi and the flow rate of 0.06 ml/min. When the suspension volume in the Amicon® container reached ~1 ml, additional 10 ml water was added into the suspension and the fractionation was continued until the volume in the container reached ~1 ml. The nanoparticle fraction that passed through the membrane and that retained on the membrane were collected separately and were lyophilized as above. For the cellular uptake studies, a formulation of nanoparticles that contained a fluorescent marker in addition to DNA was used. The dye (6-coumarin, 50 μg) was dissolved in the PLGA polymer solution prior to emulsification. Thus, the nanoparticle formulation used for the transfection studies and for the cellular uptake studies were essentially similar in composition except that the latter formulation contained the fluorescent dye. The dye serves as a sensitive marker for nanoparticles and was used in our previous studies to quantitatively determine the cellular and tissue uptake of nanoparticles (Panyam et al., 2002a; Davda and Labhasetwar, 2002).

2.2.3. Determination of particle size and surface charge of nanoparticles

The particle size of the unfractionated and the fractionated nanoparticles was determined by both dynamic light scattering technique and transmission electron microscopy (TEM). For TEM, a drop of nanoparticle suspension was placed on to the TEM grid and the particles were visualized following negative staining with 2% uranyl acetate (Electron Microscopy services, Ft. Washington, PA) using a Philips 201® TEM (Philips/FEI Inc., Briarcliff Manor, NY). Diameter of 100–150 nanoparticles from five to seven different TEM fields was measured to determine the mean particle size of nanoparticles. To measure nanoparticle size using dynamic laser light scattering, a nanoparticle suspension (0.5 mg/ml in distilled water) was subjected to particle size analysis using a Zeta Plus™ particle size analyzer (Brookhaven Instruments Corp., Holtsville, NY). Zeta potential (surface charge) of nanoparticles (0.5 mg/ml nanoparticles in water) was determined using a Zeta Plus™ zeta potential analyzer.

2.2.4. Determination of nanoparticle bound PVA

The amount of PVA associated with nanoparticles was determined using a colorimetric method described by Joshi et al. (1979). About 2 mg of lyophilized nanoparticle sample was digested in 2 ml of 0.5N NaOH for 15 min at 60 °C. The solution was neutralized with 900 µl of 1N HCl and then diluted to 5 ml with distilled water. To the above solution, 3 ml of 0.65 M boric acid, 0.5 ml of I_2/KI (0.05/0.15 M) and 1.5 ml of distilled water were added. Following incubation for 15 min at room temperature, the absorbance of the solution was measured at 690 nm using an UV spectrophotometer. The standard plot was prepared using PVA solution at different concentrations (0–30 µg/ml) that were treated similarly. The amount of PVA associated with nanoparticles was then expressed as % w/w.

2.2.5. Determination of DNA loading, encapsulation efficiency, and DNA conformation following encapsulation

The DNA loading in nanoparticles was determined from the total amount of DNA added in the formulation and the DNA amount that was not encapsulated. For this, the concentration of DNA in the washings was determined by measuring the UV absorbance at 260 nm with the washings from the control nanoparticles formulated without DNA as a blank. Direct extraction of DNA from nanoparticles was also tried by two different methods. A sample of nanoparticles was digested in 0.5N NaOH at 60 °C and the aliquots were taken at 15 min, 30 min, 1 h, 2 h, and 24 h. The aliquots were centrifuged (10 min at 4 °C and 14 000 rpm, Eppendorf® 5417R, Brinkmann Instruments, Westbury, NY) and the supernatant from each tube was assayed for the DNA levels at 260 nm using an UV spectrophotometer. The digest from control nanoparticles treated in the same manner served as a blank. In another method, a sample of nanoparticles was dissolved in chloroform and the chloroform layer was extracted repeatedly (five times) with TE buffer (pH 8.0). The DNA levels in the extract were determined as above. The DNA extracted using the above method was used to determine the conformation of the encapsulated DNA by agarose gel electrophoresis. The conformation of the DNA, which did not get encapsulated in nanoparticles and leached out in the aqueous PVA solution during their formulation, was also determined. A 20 µl aliquot of the extracted DNA and the DNA from the nanoparticle washing were loaded on to a 0.8% agarose gel in electroporation buffer with stock plasmid DNA solution as a control. The gel was visualized under UV following staining with ethidium bromide solution and photographed.

2.2.6. In vitro release of DNA from nanoparticles

In vitro release of the DNA from the larger and smaller-sized fractions of nanoparticles was studied by incubating 0.15 mg of the respective fractions with 0.5 ml of TE buffer in Eppendorf® tubes at 37 °C in an Environ Orbital Shaker (Lab Line, Melrose Park, IL) set at 100 rpm. Separate tubes were used for each data point. At predetermined time intervals, the nanoparticle suspension was centrifuged and the amount of DNA released in the supernatant was analyzed by PicoGreen® assay (Promega).

2.2.7. Transfection studies and determination of luciferase protein levels

COS-7 and HEK-293 cells were grown in DMEM supplemented with 10% FBS, 100 µg/ml penicillin G, 100 µg/ml streptomycin, and 5% MEM non-essential amino acids. For transfection studies, cells were cultured in 24-well plate 1 day prior to transfection. The transfection was carried out at ∼ 70% confluency. A nanoparticle suspension was prepared in the serum free medium (3 mg in 500 µl) using a water bath sonication for 10 min (FS140, Fisher Scientific, Pittsburgh, PA). The nanoparticle suspension was then diluted to 12 ml with complete DMEM medium. The medium in the wells was replaced with 1 ml of nanoparticle suspension (equivalent to about 6.8 µg DNA/well). The dose of nanoparticles used for the transfection was based on the preliminary dose-response study. The medium was changed on every 3rd day for HEK-293 cell line with no further addition of nanoparticles. To measure the luciferase protein levels, the cells were washed twice using 1 × phosphate buffer saline (PBS) and lysed using 1 × CCLR (Promega). To each 20 µl of the cell lysate sample, 100 µl of the reconstituted luciferase assay substrate (Promega) was added and the chemiluminiscence intensity was measured immediately using a luminometer (TD 20/20, Promega). The amount of luciferase protein was determined from the standard plot prepared using a recombinant luciferase protein. The total cell protein was determined using a BioRad® protein assay kit (BioRad, Hercules, CA) and the data were represented as luciferase protein levels in fg per mg cell protein.

2.2.8. Cellular nanoparticle uptake studies

For the cellular uptake study, a formulation of DNA loaded nanoparticles containing 6-coumarin as a fluorescent marker was used. COS-7 cells were incubated with a suspension of nanoparticles at the same dose used for the transfection study for 1 h, washed twice with 1 × PBS, and then lysed using 100 µl/well of 1 × CCLR. One hour was selected for the incubation of nanoparticles because the previous studies have shown almost a saturation uptake of nanoparticles during this time period (Davda and Labhasetwar, 2002). In-tracellular nanoparticle uptake was determined as described previously (Davda and Labhasetwar, 2002). In brief, a 5 µl aliquot of each sample was used to determine the total cell protein using BioRad® assay and the remaining portion was lyophilized for 24 h. The dye (6-coumarin) from the nanoparticles in the cell lysates was extracted by incubating each cell lysate sample with 1 ml of methanol at 37 °C for 24 h at 100 rpm in an Environ® lab shaker (Labline, Melrose Park, IL). The samples were centrifuged (14000 rpm for 10 min at 4 °C in an Eppendorf® microcentrifuge) to remove the cell debris and the supernatant from each sample was analyzed for the 6-coumarin levels using a high performance liquid chromatography (HPLC) as described in our previous studies (Davda and Labhasetwar, 2002). The uptake was represented as nanoparticle amount in µg normalized to per mg of total cell protein.

2.2.9. Statistical methods

Student t-test was used to test the significance of difference in the transfection efficiency and uptake of the smaller and the larger-sized particles. A P-value less than 0.05 was accepted as statistically significant. All data analyses were done using MINITAB® statistical software (Minitab Inc., State College, PA).

3. Results and discussion

3.1. Characterization of nanoparticles containing plasmid DNA

The unfractionated nanoparticles, when analyzed by dynamic light scattering, demonstrated a bimodal size distribution with particles in two size ranges: 95–130 nm and 330–450 nm (Fig. 1A). Following fractionation, both the fractions demonstrated unimodal particle size distribution. The fraction that passed through the membrane was designated as the smaller-sized nanoparticles and the fraction that was retained on the membrane was designated as the larger-sized nanoparticles. The smaller-sized fraction had a mean hydrodynamic diameter of 148.7 nm (polydispersity = 0.115) (Fig. 1B) while the larger-sized frac-

tion had a mean hydrodynamic diameter of 298.2 nm (polydispersity = 0.224) (Fig. 1C). Although the smaller-sized nanoparticles were passed through the membrane of 100 nm porosity, the particle size measurement showed a mean diameter larger than 100 nm by the above method. The discrepancy in the size of nanoparticles is because the dynamic light scattering method gives the hydrodynamic diameter rather than the actual diameter of nanoparticles. The particle size discrepancy is further evident from the TEM of the unfractionated and the fractionated nanoparticles.

Fig. 2. Transmission electron microscopy of fractionated smaller-sized (A) and larger-sized (B) nanoparticles. Bar represents 500 nm. Magnification 14000 × .

The mean diameter of the unfractionated nanoparticles was 97 ± 3 nm whereas that of the lower-sized fraction was 70 ± 2 nm (Fig. 2A) and the larger-sized fraction was 202 ± 9 nm (Fig. 2B). Thus the mean nanoparticle diameter measured using TEM is significantly smaller than the mean diameter obtained with the dynamic light scattering method.

The PVA associated with nanoparticles could contribute towards the hydrodynamic diameter of nanoparticles. In this study, it was found that $9.1 \pm 0.9\%$ w/w (mean $\pm$ SEM, $n = 6$) PVA remains associated with nanoparticles and is not washable. The PVA is known to form layers of aggregates (~ 5 layers) around the surface of nanoparticles contributing towards the hydrodynamic diameter of nanoparticles (Zambaux et al., 1998). Recently, we have shown that the amount of PVA bound to nanoparticles affect their physical (e.g. zeta potential, hydrophilicity) as well as cellular uptake properties. Nanoparticles with greater amount of bound PVA have been found to have reduced cellular uptake (Sahoo et al., 2002). Harvie et al. (2000) have shown that the transfection efficiency of lipid-DNA complex is reduced following conjugation of the lipid to poly (ethylene glycol). The reduced cellular uptake of the conjugated lipid–DNA complex due to steric hindrance has been attributed to the reduced transfection efficiency. In our studies, the reduced cellular uptake of nanoparticles with higher PVA
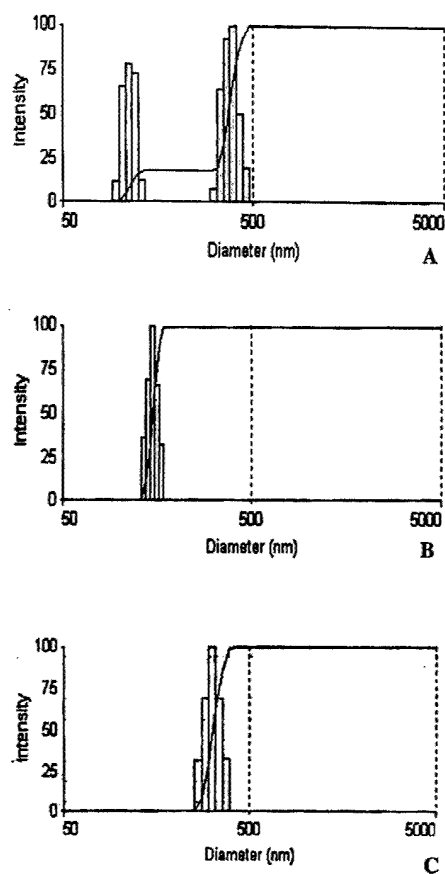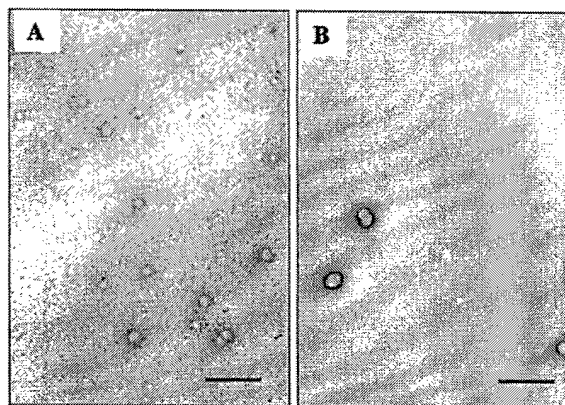

Fig. 1. Particle size distribution of (A) unfractionated nanoparticles, (B) nanoparticles passing through the membrane, and (C) nanoparticles retained on the membrane. Particle size distribution was measured by dynamic light scattering. The unfractionated nanoparticles have bimodal particle size distribution whereas fractionated nanoparticles have unimodal size distribution. The horizontal lines across the graphs represent the cumulative fraction of the total intensity of the different sized nanoparticles

bound nanoparticles has been attributed to the increase in hydrophilicity of nanoparticles with the increase in the amount of nanoparticle bound PVA. Therefore, it would be interesting to determine in the future studies the effect of nanoparticle-bound PVA on the transfection efficiency of nanoparticles.

Zeta potentials of the DNA-loaded unfractionated (-23 ± 1 mV, mean of five readings $\pm$ SEM), the smaller-sized (-20.8 ± 1.6 mV) and the larger-sized (-20.6 ± 1.5 mV) nanoparticle fractions were almost similar, suggesting that there was no difference in the surface charge characteristics of these nanoparticles. The DNA loading in the nanoparticles, as determined by the indirect method of analysis, was 2.1–2.7% w/w with an entrapment efficiency of 78–83%. The loading represents the amount of DNA present per unit weight of nanoparticles whereas the efficiency of entrapment represents the percent of the total added DNA that has been entrapped into nanoparticles. Attempts to determine the DNA loading in nanoparticles by direct methods were not successful either because the DNA degraded under the conditions used for digesting the nanoparticles or due to the precipitation of PLGA–PVA complex along with DNA at the organic solvent–TE buffer interface resulting in the incomplete extraction of DNA. The above

problem of extraction of macromolecules especially from nanoparticles has been reported by other investigators (Cohen et al., 2000), and hence the indirect method of DNA loading is commonly used to overcome the problem (Perez et al., 2001; Klugherz et al., 2000).

The DNA that leached out in the washings and that extracted from nanoparticles showed bands corresponding to that of the supercoiled and circular forms of DNA (Fig. 3A and B). The results thus suggest that sonication did not cause the fragmentation of DNA during the formulation of nanoparticles, and the DNA was probably protected due to its encapsulation within the polymer in the emulsion. Sonication of DNA in solution under similar conditions resulted in a complete fragmentation of DNA. Protection of the DNA structure during emulsification is important as fragmentation of DNA could affect the transfectivity of nanoparticles (Walter et al., 1999). While there was some open circular form of the DNA present in the stock, agarose gel electrophoresis results show that the encapsulation results in a partial transformation of DNA from the supercoiled to the open circular form. This partial transformation of DNA following encapsulation has been reported for PLGA microspheres and has been attributed to the encapsulation procedure (homogenization) and lyophilization (Ando
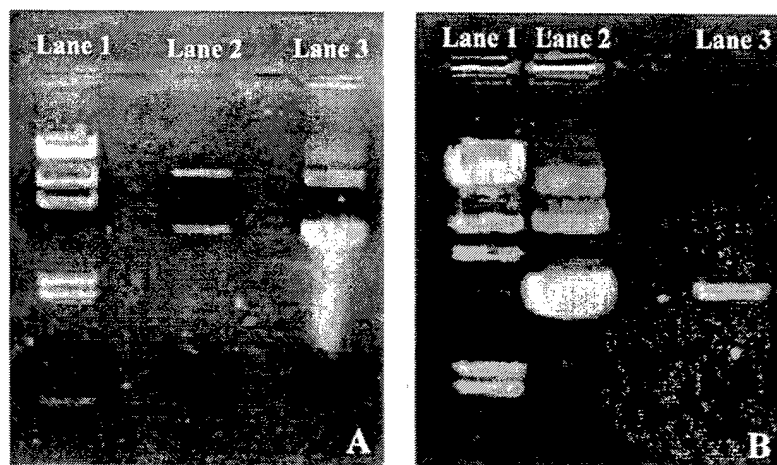

Fig. 3. Agarose gel electrophoresis of DNA extracted from nanoparticles (A) (lane 1: molecular weight markers, lane 2: extracted DNA, lane 3: stock plasmid DNA) and from nanoparticle washings (B) (lane 1: molecular weight markers, lane 2: stock plasmid DNA, lane 3: nanoparticle washings).

et al., 1999). Similar transformation of the DNA following encapsulation has been reported by other investigators also (Cohen et al., 2000; Cherng et al., 1999; Bergan et al., 2000). However, this partial transformation of DNA is not expected to affect the transfectivity of nanoparticles as Cohen et al. (2000) have demonstrated that the difference in the transfection levels of the supercoiled and relaxed forms of the DNA extracted from nanoparticles is statistically insignificant. Also, in another study, it was demonstrated that DNA in supercoiled or relaxed form formulated with cationic lipids do not show any significant difference in the transfection efficiency in cell culture (Bergan et al., 2000).

3.2. Effect of particle size on transfection, DNA release, and cellular uptake

The transfection studies in COS-7 showed a 27-fold higher luciferase protein levels for the fractionated smaller-sized nanoparticles as compared to the larger-sized nanoparticles ($P < 0.05$, $n = 6$) or the unfractionated particles (Fig. 4A) for the same dose of nanoparticles. The fact that the fraction of the smaller-sized particles is significantly lower in the unfractionated nanoparticle preparation (less than 5% by weight) may explain the similar transfection levels observed for the unfractionated and the larger-sized nanoparticles (Fig. 4A). In the transfection studies, however, equal weight of the smaller-sized and the larger-sized nanoparticles was used and hence the difference in the transfectivity of the two sized nanoparticles could be seen. The transfection studies in COS-7 cells could not be continued beyond 2 days because the cells reached confluency and began to detach.

In HEK-293 cell line, the smaller-sized nanoparticles showed a 4-fold higher transfection as compared to the larger-sized nanoparticles ($P < 0.05$, $n = 6$) (Fig. 4B). The transfection level increased slowly and reached a peak in 5–7 days post-transfection. The cells started detaching thereafter and hence the transfection studies could not be continued beyond 1 week. The sustained gene expression in HEK-293 cells seems to be due to the slow release of DNA from the nanoparti-
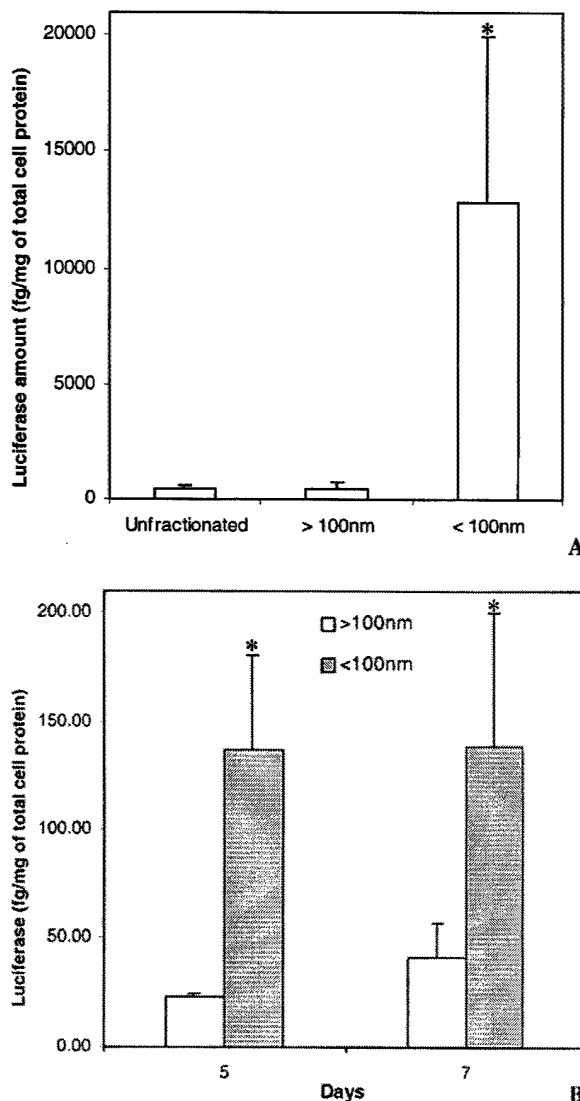

Fig. 4. (A) Transfection with unfractionated and fractionated smaller- and larger-sized nanoparticles in COS-7 cell line. The luciferase protein levels were measured two days after the transfection. Results are expressed as mean ± SEM ($n = 6$, * $P < 0.05$ compared to larger-sized and unfractionated nanoparticles). (B) Transfection with fractionated smaller- and larger-sized nanoparticles in HEK-293 cell line. The luciferase protein levels were measured at 5 and 7 days post-transfection. Results are expressed as mean ± SEM ($n = 6$, * $P < 0.05$ compared to larger-sized nanoparticles).

cles. Similar studies using FuGene™6 (Roche Diagnostic, Indianapolis, IN), a commercially available transfecting agent, showed peak luciferase level at 2 days, which then rapidly declined

(data not shown), supporting our hypothesis of sustained gene expression using nanoparticles.

Further, about 165-fold difference (78 ± 30.5 fg/mg in HEK-293 vs. 12805 ± 7128 fg/mg in COS-7 for smaller-sized nanoparticles) in the transfection levels observed in the two cell lines, for the same dose of nanoparticles and for the same duration (2 days) of transfection, suggests that the nanoparticle-mediated gene transfection is cell line-dependent. The cell line-dependent variation in transfection levels has also been reported for other gene delivery systems. It is possible that COS-7 is a relatively rapidly dividing cell line compared to HEK-293, and hence there is greater nuclear uptake of DNA released from nanoparticles in COS-7 than in HEK-293 during cell division. The above possibility has been suggested for cationic lipid-mediated gene transfer (Escriou et al., 2001).

In order to determine the mechanism of higher transfectivity of the smaller-sized nanoparticles compared to that of the larger-sized nanoparticles, we determined the DNA release from the two fractions of nanoparticles and their cellular uptake in COS-7 cells. The DNA release study shows that the larger-sized nanoparticles have slightly higher extent of DNA release than from an equal weight of the smaller-sized nanoparticles (Fig. 5). In this study, the release study was carried out for 7 days because the transfection study was carried out for a maximum period of 7 days. However, in our previous study, a sustained release of DNA from PLGA nanoparticles was demonstrated with a 26% cumulative release occurring in the 1st hour as a burst phase, followed by a gradual elution with a 82% cumulative release in 17 days (Labhasetwar et al., 1999). Similar sustained DNA release pattern for PLGA nano- and microparticles has been reported by other investigators (Wang et al., 1999; Cohen et al., 2000). Based on the in vitro release study, the available DNA for transfection is not significantly different for the two fractions of nanoparticles and does not seem to be the factor responsible for higher transfection observed with the smaller-sized nanoparticles. The cellular uptake study demonstrated that the uptake of the smaller- and the larger-sized nanoparticles were almost similar

(33.2 ± 6.5 μg nanoparticles/mg vs. 27.5 ± 4.7 μg nanoparticles/mg of total cell protein, respectively, mean $\pm$ SEM, $n = 6$, $P > 0.05$).

Since the surface charge (zeta potential), cellular uptake, and the DNA release were almost similar for the two fractions of nanoparticles, these factors do not seem to be responsible for the observed differences in the transfection levels. One of the possible reasons for the observed higher transfection efficiency for the smaller-sized fraction could be due to the difference in the total number of particles present in the cells for the same mass of nanoparticles taken up. Based on the mean particle diameter of the two fractions of nanoparticles and the above cellular uptake data, it could be estimated that the number of the smaller-sized nanoparticles taken up by the cells would be about 20-fold greater than the larger-sized nanoparticles (350×10^8 vs. 17×10^8 per mg cell protein for smaller- and larger-sized nanoparticles, respectively) (Müller, 1991).

Various investigators have reported the importance of size of plasmid DNA and DNA carriers for gene transfection (Kreiss et al., 1999; Cherng et al., 1999). Plasmid DNA of smaller size was previously shown to have higher transfection efficiency. It was suggested that the greater extent of
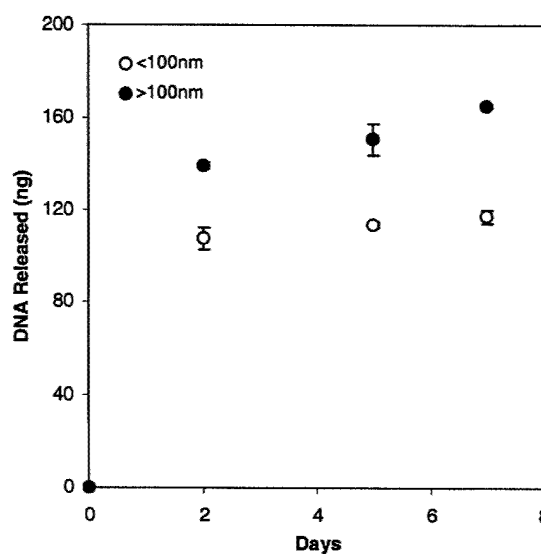

Fig. 5. In vitro release of DNA from smaller-sized and larger-sized nanoparticles. Data as mean $\pm$ SEM ($n = 3$).

the DNA release from cationic lipids as compared to that from larger size DNA complexes, or greater intracellular migration of smaller size DNA from cytoplasm to nucleus or both of the above mechanisms could be responsible for the observed higher transfection of the smaller size DNA (Kreiss et al., 1999). Cherng et al. have reported that the optimal transfection efficiency of the poly ((2-dimethylamino) ethyl methacrylate) (PDMAEMA)-plasmid particles was at PDMAEMA-plasmid ratio of 3 (w/w) containing slightly positively charged particles with a narrow size distribution and average diameter of 150 nm. However, PDMAEMA-plasmid ratios less than 1.5 (w/w) resulted in rather large particles with high polydispersity index. In their study, it has been suggested that the larger particles are too voluminous to be taken up by the cell via endocytosis resulting in lower transfection. Future studies aimed at investigating the intracellular distribution of the two fractions of nanoparticles could reveal the reason for the observed difference in the transfection efficiency of the two different nanoparticle fractions.

4. Conclusions

In this study, we have shown that the double-emulsion solvent evaporation technique commonly used for PLGA nanoparticle formulation results in a heterogeneous particle-size distribution and that the smaller-sized fraction of nanoparticles (< 100 nm) has significantly higher transfection efficiency as compared to the larger-sized fraction of nanoparticles (> 100 nm). The greater transfection of the smaller-sized fraction as compared to the larger-sized fraction of nanoparticles does not seem to be related to their surface properties (zeta potential), cellular uptake or the rate and extent of release of DNA. Although the method used in this study to fractionate nanoparticles may not be commercially practical since it provides low yield (less than 5% on weight basis) of the smaller-sized nanoparticles, the results of the study are important because they signify the importance of particle size in nanoparticle-mediated gene transfection. The re-

sults suggest that formulating nanoparticles of smaller diameter is critical to improving the efficiency of nanoparticle-mediated transfection.

References

Ando, S., Putnam, D., Pack, D.W., Langer, R., 1999. PLGA microspheres containing plasmid DNA: Preservation of supercoiled DNA via cryopreparation and carbohydrate stabilization. J. Pharm. Sci. 88, 126–130.

Bergan, D., Galbraith, T., Sloane, D.L., 2000. Gene transfer in vitro and in vivo by cationic lipids is not significantly affected by levels of supercoiling of a reporter plasmid. Pharm. Res. 17, 967–973.

Bonadio, J., Smiley, E., Patil, P., Goldstein, S., 1999. Localized, direct plasmid gene delivery in vivo: prolonged therapy results in reproducible tissue regeneration. Nat. Med. 5, 753–759.

Cherng, J.Y., Schuurmans-Nieuwenbroek, N.M., Jiskoot, W., Talsma, H., Zuidam, N.J., Hennink, W.E., Crommelin, D.J., 1999. Effect of DNA topology on the transfection efficiency of poly((2-dimethylamino)ethyl methacrylate)-plasmid complexes. J. Control. Release 60, 343–353.

Clark, K.R., Johnson, P.R., 2001. Gene delivery of vaccines for infectious disease. Curr. Opin. Mol. Ther. 3, 375–384.

Cohen, H., Levy, R.J., Gao, J., Fishbein, I., Kousaev, V., Sosnowski, S., Slomkowski, S., Golomb, G., 2000. Sustained delivery and expression of DNA encapsulated in polymeric nanoparticles. Gene Ther. 7, 1896–1905.

Dauty, E., Remy, J.S., Blessing, T., Behr, J.P., 2001. Dimerizable cationic detergents with a low cmc condense plasmid

DNA into nanometric particles and transfect cells in culture. J. Am. Chem. Soc. 123, 9227–9234.

Davda, J., Labhasetwar, V., 2002. Characterization of nanoparticle uptake by endothelial cells. Int. J. Pharm. 233, 51–59.

Desai, M.P., Labhasetwar, V., Walter, E., Levy, R.J., Amidon, G.L., 1997. The mechanism of uptake of biodegradable microparticles in Caco-2 cells is size dependent. Pharm. Res. 14, 1568–1573.

Escriou, V., Carriere, M., Bussone, F., Wils, P., Scherman, D., 2001. Critical assessment of the nuclear import of plasmid during cationic lipid-mediated gene transfer. J. Gene Med. 3, 179–187.

Harvie, P., Wong, F.M., Bally, M.B., 2000. Use of poly(ethylene glycol)-lipid conjugates to regulate the surface attributes and transfection activity of lipid-DNA particles. J. Pharm. Sci. 89, 652–663.

Hedley, M.L., Curley, J., Urban, R., 1998. Microspheres containing plasmid-encoded antigens elicit cytotoxic T-cell responses. Nat. Med. 4, 365–368.

Joshi, D.P., Lan-Chun-Fung, Y.L., pritchard, J.G., 1979. Determination of poly vinyl alcohol via its complex with boric acid and iodine. Anal. Chim. Acta 104, 153–160.

Kataoka, K., Harashima, H., 2001. Gene delivery systems: viral vs. non-viral vectors. Adv. Drug Deliv. Rev. 52, 151.

Klugherz, B.D., Jones, P.L., Cui, X., Chen, W., Meneveau, N.F., DeFelice, S., Connolly, J., Wilensky, R.L., Levy, R.J., 2000. Gene delivery from a DNA controlled-release stent in porcine coronary arteries. Nat. Biotechnol. 18, 1181–1184.

Kochanek, S., Schiedner, G., Volpers, C., 2001. High-capacity 'gutless' adenoviral vectors. Curr. Opin. Mol. Ther. 3, 454–463.

Kreiss, P., Cameron, B., Rangara, R., Mailhe, P., Aguerre-Charriol, O., Airiau, M., Scherman, D., Crouzet, J., Pitard, B., 1999. Plasmid DNA size does not affect the physicochemical properties of lipoplexes but modulates gene transfer efficiency. Nucleic Acids Res. 27, 3792–3798.

Labhasetwar, V., Bonadio, J., Goldstein, S., Levy, R.J., 1999. Gene transfection using biodegradable nanospheres: results in tissue culture and a rat osteotomy model. Colloids Surfaces B: Biointerfaces 16, 281–290.

Lee, H., Williams, S.K., Allison, S.D., Anchordoquy, T.J., 2001. Analysis of self-assembled cationic lipid–DNA gene carrier complexes using flow field-flow fractionation and light scattering. Anal. Chem. 73, 837–843.

Li, S., Huang, L., 2000. Nonviral gene therapy: promises and challenges. Gene Ther. 7, 31–34.

Luo, D., Woodrow-Mumford, K., Belcheva, N., Saltzman, W.M., 1999. Controlled DNA delivery systems. Pharm. Res. 16, 1300–1308.

Maheshwari, A., Mahato, R.I., McGregor, J., Han, S., Samlowski, W.E., Park, J.S., Kim, S.W., 2000. Soluble biodegradable polymer-based cytokine gene delivery for cancer treatment. Mol. Ther. 2, 121–130.

Mao, H.Q., Roy, K., Troung-Le, V.L., Janes, K.A., Lin, K.Y., Wang, Y., August, J.T., Leong, K.W., 2001. Chitosan-DNA nanoparticles as gene carriers: synthesis, characterization and transfection efficiency. J. Control. Release 70, 399–421.

Müller, R.H., 1991. Colloidal Carriers for Controlled Drug Delivery and Targeting. CRC press, Boca Raton.

Ohno, T., Gordon, D., San, H., Pompili, V.J., Imperiale, M.J., Nabel, G.J., Nabel, E.G., 1994. Gene therapy for vascular smooth muscle cell proliferation after arterial injury. Science 265, 781–784.

Panyam, J., Lof, J., O'Leary, E., Labhasetwar, V., 2002a. Efficiency of Dispatch® and Infiltrator® cardiac infusion catheters in arterial localization of nanoparticles in a porcine coronary model of restenosis. J. Drug Target, in press.

Panyam, J., Zhou, W.Z., Prabha, S., Sahoo, S.K., Labhasetwar, V., 2002b. Rapid endolysosomal escape of poly (D,L-lactide-co-glycolide) nanoparticles: Implications for drug and gene delivery. FASEB J., in press.

Perez, C., Sanchez, A., Putnam, D., Ting, D., Langer, R., Alonso, M.J., 2001. Poly(lactic acid)-poly(ethylene glycol) nanoparticles as new carriers for the delivery of plasmid DNA. J. Control. Release 75, 211–224.

Richardson, T.P., Peters, M.C., Ennett, A.B., Mooney, D.J., 2001. Polymeric system for dual growth factor delivery. Nat. Biotechnol. 19, 1029–1034.

Roy, K., Mao, H.Q., Huang, S.K., Leong, K.W., 1999. Oral gene delivery with chitosan—DNA nanoparticles generates immunologic protection in a murine model of peanut allergy. Nat. Med. 5, 387–391.

Rubanyi, G.M., 2001. The future of human gene therapy. Mol. Aspects Med. 22, 113–142.

Sahoo, S.K., Panyam, J., Prabha, S., Labhasetwar, V., 2002. Residual polyvinyl alcohol associated with poly (D,L-lactide-co-glycolide) nanoparticles affects their physical properties and cellular uptake. J. Control. Release 82, 105–114.

Sakurai, F., Inoue, R., Nishino, Y., Okuda, A., Matsumoto, O., Taga, T., Yamashita, F., Takakura, Y., Hashida, M., 2000. Effect of DNA/liposome mixing ratio on the physicochemical characteristics, cellular uptake and intracellular trafficking of plasmid DNA/cationic liposome complexes and subsequent gene expression. J. Control. Release. 66, 255–269.

Truong-Le, V.L., August, J.T., Leong, K.W., 1998. Controlled gene delivery by DNA-gelatin nanospheres. Hum. Gene Ther. 9, 1709–1717.

Walter, E., Moelling, K., Pavlovic, J., Merkle, H.P., 1999. Microencapsulation of DNA using poly(DL-lactide-co-glycolide): stability issues and release characteristics. J. Control. Release 61, 361–374.

Wang, D., Robinson, D.R., Kwon, G.S., Samuel, J., 1999. Encapsulation of plasmid DNA in biodegradable poly(D,L-lactic-co-glycolic acid) microspheres as a novel approach for immunogene delivery. J. Control. Release 57, 9–18.

Zambaux, M.F., Bonneaux, F., Gref, R., Maincent, P., Dellacherie, E., Alonso, M.J., Labrude, P., Vigneron, C., 1998. Influence of experimental parameters on the characteristics of poly(lactic acid) nanoparticles prepared by a double emulsion method. J. Control. Release 50, 31–40.

Zauner, W., Farrow, N.A., Haines, A.M., 2001. In vitro uptake of polystyrene microspheres: effect of particle size, cell line and cell density. J. Control. Release 71, 39–51.

Rapid endo-lysosomal escape of poly(DL-lactide-co-glycolide) nanoparticles: implications for drug and gene delivery

JAYANTH PANYAM,* WEN-ZHONG ZHOU,* SWAYAM PRABHA,*
SANJEEB K. SAHOO,* AND VINOD LABHASETWAR*,†,1

*Department of Pharmaceutical Sciences, University of Nebraska Medical Center,
Omaha, Nebraska 68198, USA, and †Department of Biochemistry and Molecular
Biology, University of Nebraska Medical Center, Omaha, Nebraska 68198, USA

ABSTRACT   The endo-lysosomal escape of drug carriers is crucial to enhancing the efficacy of their macromolecular payload, especially the payloads that are susceptible to lysosomal degradation. Current vectors that enable the endo-lysosomal escape of macromolecules such as DNA are limited by their toxicity and by their ability to carry only limited classes of therapeutic agents. In this paper, we report the rapid (<10 min) endo-lysosomal escape of biodegradable nanoparticles (NPs) formulated from the copolymers of poly(DL-lactide-co-glycolide) (PLGA). The mechanism of rapid escape is by selective reversal of the surface charge of NPs (from anionic to cationic) in the acidic endo-lysosomal compartment, which causes the NPs to interact with the endo-lysosomal membrane and escape into the cytosol. PLGA NPs are able to deliver a variety of therapeutic agents, including macromolecules such as DNA and low molecular weight drugs such as dexamethasone, intracellularly at a slow rate, which results in a sustained therapeutic effect. PLGA has a number of advantages over other polymers used in drug and gene delivery including biodegradability, biocompatibility, and approval for human use granted by the U.S. Food and Drug Administration. Hence PLGA is well suited for sustained intracellular delivery of macromolecules.—Panyam, J., Zhou, W. Z., Prabha, S., Sahoo, S. K., Labhasetwar, V. Rapid endo-lysosomal escape of poly(DL-lactide-co-glycolide) nanoparticles: implications for drug and gene delivery. FASEB J. 16, 1217–1226 (2002)

Key Words: intracellular delivery · gene therapy · antiproliferative effect · sustained release · restenosis

DEVELOPMENT OF AN efficient therapy based on macromolecular drugs such as genes and proteins depends on their safe and efficient intracellular delivery. However, a number of barriers exist for the cellular entry of these macromolecules including the poor permeability and selectivity of cell membranes and degradation of the macromolecules in the lysosomes following their internalization by endocytosis (1, 2). Thus, in recent years there has been significant interest in developing carriers for intracellular delivery that will enable a variety of macromolecules to escape the degradative endo-lysosomal compartment and result in their efficient intracellular delivery (3, 4).

Endo-lysosomal escape has been reported for a number of vectors used in gene therapy including viruses, fusogen peptides, cationic lipids, and cationic polymers. Viruses and peptide toxins use a fusogen peptide to cross the endosomal membrane and reach the cytosol (5). Nonviral vectors such as cationic lipids and polycations protect the DNA by either retarding the transfer of DNA from endosomes to lysosomes or destabilizing the endo-lysosomal membranes (2). However, these carriers suffer from a number of limitations including immunogenicity, toxicity, instability in vivo, and the ability to deliver only DNA or oligonucleotides (6).

A number of small protein domains, termed protein transduction domains (PTDs), can cross biological membranes without the necessity of endocytosis and have been shown to be useful for carrying various peptides and proteins into cells (7). However, these PTD vectors have a certain number of limitations in that they all require cross-linking to the target peptide or protein (8). Also, some of these systems such as PTDs derived from HIV-1 TAT protein require denaturation of the protein before delivery to increase the accessibility of the TAT-PTD domain (9). More recently, a short amphipathic carrier, Pep-1, was used to deliver functionally active proteins and peptides intracellularly without the need for cross-linking or denaturation (8). However, most of these vectors are also constrained by their ability to carry only protein or peptide therapeutics. Thus, there is a need for a carrier that is nontoxic and biodegradable and that has the ability to deliver intracellularly multiple classes of therapeutic agents.

We report here one such system, polymeric nanoparticles (NPs) formulated from the biodegradable polymer poly(DL-lactide-co-glycolide) (PLGA), that is able to cross the endosomal barrier and deliver the encapsulated therapeutic agents into the cytoplasm. NPs are

---

colloidal systems that typically range in diameter from 10 to 1000 nm, with the therapeutic agent either entrapped into or adsorbed or chemically coupled onto the polymer matrix (10). The PLGA NP formulation with a therapeutic agent entrapped into the polymer matrix provides sustained drug release. The degradation products of PLGA are lactic and glycolic acids that are formed at a very slow rate and are easily metabolized in the body via the Krebs cycle and are eliminated (11). PLGA has previously been used for drug, protein, and gene delivery applications because of its biocompatibility and sustained-release properties (12–15). Thus, PLGA NPs offer the advantages of safety, the ability to carry different classes of therapeutic agents, and the possibility of sustained intracytoplasmic delivery. In this report, we demonstrate the rapid endolysosomal escape of PLGA NPs. We further demonstrate a sustained therapeutic effect of an NP-encapsulated low molecular weight drug with cytoplasmic receptor (dexamethasone) and sustained gene expression with DNA-loaded NPs as an example of a macromolecular therapeutic agent.

MATERIALS AND METHODS

Materials

LysoTracker Red and Texas Red-conjugated transferrin were purchased from Molecular Probes (Eugene, OR). Fluoresbrite YG NPs (mean diameter 84 ± 10 nm) and 6-coumarin were purchased from Polysciences (Warrington, PA). PLGA was purchased from Birmingham Polymers (Birmingham, AL). All the reagents used for transmission electron microscopy (TEM) were from Electron Microscopy Services (Ft. Washington, PA). Other chemicals and reagents were purchased from Sigma (St. Louis, MO).

NP formulation

NPs containing a fluorescent dye, 6-coumarin (fluorescent NPs), were formulated by using a double emulsion-solvent evaporation technique as described previously (16). In a typical procedure, a solution of bovine serum albumin (BSA) (60 mg in 1 ml of water) was emulsified in polymer (PLGA 50:50, molecular weight 143,000) solution (180 mg in 6 ml of chloroform) containing 6-coumarin (100 µg) using a probe sonicator (55 W for 2 min) (Sonicator XL, Misonix, Farmingdale, NY). BSA was used as a model macromolecule in the formulation of fluorescent NPs. The water-in-oil emulsion thus formed was further emulsified into 50 ml of 2.5% w/v aqueous solution of polyvinyl alcohol (PVA) used as an emulsifier by using sonication as above for 5 min to form a multiple water-in-oil-in-water emulsion. NPs containing plasmid DNA (pGL3 containing the firefly luciferase cDNA downstream of the SV40 promoter) were prepared by an identical procedure except that the DNA solution in Tris-EDTA buffer (0.6 ml, 10 mg/ml) was used to form the primary emulsion. NPs containing osmium tetroxide, an electron-dense agent, were formulated similarly, except that 10 mg of osmium tetroxide, instead of 6-coumarin, was added to the polymer solution. Dexamethasone-loaded NPs were formulated by emulsifying the polymer solution containing dexamethasone (50 mg of PLGA and 8 mg of dexamethasone

dissolved in a mixture of 2 ml of chloroform and 0.5 ml of acetone) into a PVA solution (10 ml of 2.5% w/v) by sonication for 10 min as above to form an oil-in-water emulsion. In general, in all the formulation procedures, the emulsion was stirred for about 18 h at room temperature followed by desiccation for 1 h in a desiccator under vacuum to evaporate chloroform. NPs thus formed were recovered by ultracentrifugation (25,000 rpm for 20 min at 4°C, Optima LE-80K, Beckman, Palo Alta, CA), washed two times to remove PVA and unentrapped agent, and then lyophilized (Sentry, Virtis, Gardiner, NY) for 48 h to obtain a dry powder.

NP characterization

NPs were evaluated for size by TEM and for surface charge (zeta potential) by using a zeta potential analyzer (ZetaPlus, Brookhaven Instruments, Holtsville, NY). For TEM, a sample of NPs was suspended in water (0.5 mg/ml) and the particles were visualized by using a Philips 201 (Philips/FEI, Briarcliff Manor, NY) transmission electron microscope after negative staining of NPs with 2% w/v uranyl acetate.

Cell culture

Human arterial smooth muscle cells (HASMCs; Cascade Biologics, Portland, OR) were used for studying the cellular uptake of NPs, although human aortic vascular smooth muscle cells (HA-VSMCs, American Type Culture Collection [ATCC], Manassas, VA) were used for antiproliferative studies. VSMCs were selected for these studies because they have been implicated in the development of restenosis and have been used as an in vitro model for studying the antiproliferative efficacy of different therapeutic agents (17). HASMCs were maintained on Medium 231 supplemented with smooth muscle growth supplement (Cascade Biologics). HA-VSMCs were maintained on Ham's F12-K medium supplemented with 10 mM 4-(2-hydroxyethyl)-1-piperazineethanesulfonic acid (HEPES), 10 mM N-tris[hydroxymethyl]methyl-2-aminoethane sulfonic acid (TES), 50 µg/ml ascorbic acid, 10 µg/ml transferrin, 10 µg/ml insulin, 10 ng/ml sodium selenite, and 30 µg/ml endothelial growth supplement, 10% FBS, 100 µg/ml penicillin G, and 100 µg/ml streptomycin (GIBCO BRL, Grand Island, NY). PC3 (prostate cancer) cells (ATCC) were grown in RPMI 1640 supplemented with 10% FBS, 100 µg/ml penicillin G, and 100 µg/ml streptomycin. We selected these cell lines because of our interest in developing NP-based drug and gene therapies for cancer and restenosis.

Cellular NP uptake studies

HASMCs were seeded at 50,000 cells/ml per well in 24-well plates (Falcon, Becton Dickinson, Franklin Lakes, NJ) and were allowed to attach for 24 h. To determine the NP uptake, the cells were incubated with a suspension of NPs in growth medium for 1 h, washed three times with PBS (pH 7.4, 154 mM), and lysed by incubating cells with 0.1 ml of 1X cell culture lysis reagent (Promega, Madison, WI) for 30 min at 37°C. The cell lysates were processed to determine the NP levels as per our previously published method (16). The fluorescent dye (6-coumarin) incorporated in PLGA NPs (~0.05% loading) is lipophilic and therefore remains associated with the polymer matrix of NPs. The dye does not leach from the NPs during the experimental period and therefore the fluorescence seen in the cells is due to NPs. Thus, the dye in NPs serves as a sensitive marker to quantitatively determine their cellular uptake and also to study their intracellular and

tissue distribution by confocal or fluorescence microscopy (16, 18).

Initially, the dose- and time-dependent cellular uptake of NPs was determined. To study the effect of various inhibitors on NP uptake, cells were preincubated first with inhibitors and then with a suspension of NPs (100 µg/ml), which also contained the respective inhibitor at the same concentration as that used for preincubation: 1) 0.1% w/v sodium azide and 50 mM 6-deoxyglucose for 1 h, 2) 10 mM ammonium chloride for 1 h, 3) 450 mM sucrose for 1 h, 4) 5 µM brefeldin A for 5 min, 5) 30 µM cytochalasin D for 30 min, 6) 33 µM nocodazole for 30 min, 7) 100 nM bafilomycin A_1 for 30 min, and 8) 1 µg/ml filipin for 30 min. To study the effect of temperature on NP uptake, cells were preincubated for 1 h at 4°C and then with an NP suspension for an additional 1 h at 4°C. Confocal microscopy and TEM were used to monitor the cellular uptake and intracellular trafficking of NPs.

Microscopic studies

For confocal microscopy, HASMCs were plated 24 h prior to the experiment in Bioptechs plates (Bioptechs, Butler, PA) at 50,000 cells/plate in 1 ml of growth medium. To study the effect of various inhibitors on the intracellular distribution of NPs, the cells were first pretreated with inhibitors and then were incubated with a suspension of fluorescent NPs (100 µg/ml) containing 50 nM LysoTracker Red and the respective inhibitor for 30 min. For the experiments involving Texas Red transferrin, cells were preincubated with serum-free growth medium for 30 min followed by treatment with a suspension of fluorescent NPs (100 µg/ml) prepared in serum-free growth medium containing Texas Red transferrin (100 µg/ml). After the cells were incubated with NPs for 30 min, they were washed twice with PBS and visualized with HEPES buffer (pH 8). The images captured by use of a 488-nm filter (fluorescein), 568-nm filter (rhodamine), and differential interference contrast using a Zeiss Confocal microscope LSM410 equipped with argon-krypton laser (Carl Zeiss Microimaging, Thornwood, NY) were overlaid to obtain images to determine localization of NPs in endo-lysosomal compartments (using LysoTracker Red as a marker), or in early and recycling endosomes (using Texas Red transferrin as a marker).

For TEM, HASMCs were plated 24 h prior to the experiment in 100-mm tissue culture dishes (Becton Dickinson) at 500,000 cells/dish in 10 ml of growth medium. To study the time-dependent cellular uptake and intracellular distribution of NPs, the cells were incubated with the osmium tetroxide-loaded NPs (100 µg/ml), were washed twice with PBS at different time points (10 min, 30 min, and 1 h postincubation) for the time-dependent uptake study, and then were harvested by trypsinization. The harvested cells were fixed in a 2.5% glutaraldehyde solution in PBS and then postfixed in 1% osmium tetroxide in PBS for 1 h. The cells were washed with PBS and dehydrated three times in a graded series of ethanol solutions (50%, 70%, 90%, 95%, 100%); they were then soaked overnight in a 1:1 ratio of 100% ethyl alcohol and Unicryl embedding resin (Ted Pella, Redding, CA), after which they were soaked in fresh Unicryl resin for 4–5 h. The cells in fresh Unicryl resin were then placed in BEEM capsules (Electron Microscopy Services), and the capsules were placed in a Pelco UV-2 Cryo Chamber (Ted Pella) at 4°C for 48 h for polymerization of the resin by UV radiation. The polymerized blocks were sectioned, and the sections (80–100 nm thick) were placed on Formvar-coated copper grids (150 mesh, Ted Pella), stained with an aqueous solution of 2% uranyl acetate for 15 min, washed briefly in water, stained with Reynolds lead citrate for 7 min, and then finally washed

in water prior to visualization under a Philips 410LS microscope (Philips/FEI).

In vitro antiproliferative studies

HA-VSMCs were plated overnight in 96-well plates at 2500 cells/well and had their growth synchronized by serum depletion for 24 h. Cells were then restimulated with normal growth medium containing 10% FBS. The growth medium also contained 10 µM dexamethasone either in solution or encapsulated in NPs. Plain growth medium and control NPs (no drug) were used as respective controls. Cell proliferation was followed by a standard MTS assay (CellTiter 96 AQ$_{ueous}$, Promega).

In vitro gene expression studies

PC-3 cells were seeded in 24-well plates 24 h prior to transfection. The transfection was carried out at 60–70% confluency. The growth medium in the wells was replaced with a suspension of the DNA-loaded NPs prepared in the growth medium containing serum. Luciferase activity was measured by using an assay kit from Promega, and the data were normalized to per milligram of cell protein. The transfection study could not be continued beyond 3 days because by then the cells had reached full confluency and started to detach.

Statistical analysis

The two-tailed unpaired Student's t test was used to analyze the significance of differences in mean responses between the various treatment groups. Differences were accepted as significant at P values < 0.05.

RESULTS

NP characterization

PLGA NPs containing 6-coumarin had a mean size of 69 ± 4 nm (mean ± SE of particles counted from 10 TEM fields) (Fig. 1A), with an average zeta potential of −12.5 ± 0.4 mV (mean ± SE, $n = 5$) at pH 7 in 0.001 M HEPES buffer (Fig. 1B). The zeta potential and the particle size of the different NP formulations are shown in **Table 1**.

Mechanism of NP uptake

The NP uptake by HASMCs was linear at lower doses of NPs (10–100 µg), but the efficiency of uptake was reduced at higher doses. The NP uptake was relatively rapid during the first 2 h of incubation, before a saturation uptake was achieved in 4–6 h. NP uptake was energy dependent, as evidenced by the reduction in the uptake by 78% and 67% at a lower temperature of incubation (4°C) and after energy depletion by a mixture of sodium azide and 6-deoxyglucose, respectively (**Fig. 2A**). Inhibition of clathrin-coated pit endocytosis by hypertonic growth medium decreased the intracellular uptake of NPs by 40%, whereas inhibition of caveola-coated pit endocytosis by filipin did not affect NP uptake, indicating that caveolae were not
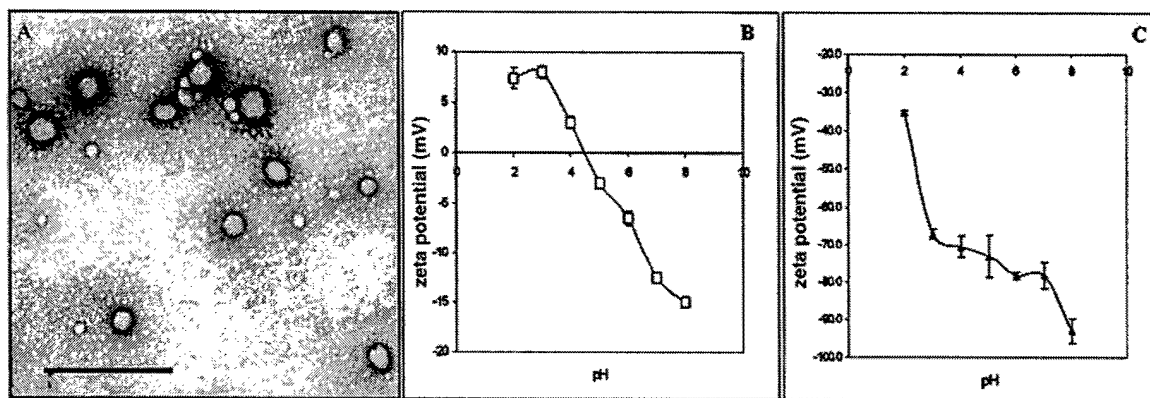
Figure 1. NP characterization: TEM of PLGA NPs (scale bar = 500 nm) (*A*), zeta potential of PLGA NPs (*B*), and zeta potential of polystyrene-NPs (*C*). Zeta potential was measured at an NP concentration of 200 μg/ml in 0.001 M HEPES buffer adjusted to different pH values with either 0.1 N sodium hydroxide or 0.1 N hydrochloric acid (mean ± SE, *n* = 5).

involved in NP uptake (Fig. 2*B*). NP uptake was not affected by cytochalasin D, a potent inhibitor of actin polymerization, which suggests that microfilaments did not play an important role in the uptake of NPs, at least in this cell line (Fig. 2*B*). However, inhibition of microtubules by nocodazole resulted in a 66% increase in NP uptake, indicating that microtubules may be involved in controlling intracellular uptake of NPs (Fig. 2*B*).

Intracellular distribution and endo-lysosomal escape of NPs

Because transferrin is a marker of early and recycling endosomes (19), we studied the colocalization of Texas Red-conjugated transferrin (red fluorescence) with fluorescent PLGA NPs (green fluorescence). This resulted in a partial colocalization (yellow fluorescence) in the peripheral cytoplasmic compartment (**Fig. 3***A*). However, NPs appeared to accumulate in compartments separate from the transferrin-labeled compartments, which suggests that a majority of NPs may be present either in late endosomes/lysosomes or in the cytoplasm. To determine whether the NPs are localized in the secondary endosomal and lysosomal compartments, cells were incubated with NPs in the presence of LysoTracker Red, a marker for secondary endosomes and lysosomes. The LysoTracker Red, which is colorless at physiological pH, has red fluorescence at the acidic pH present in these compartments. As shown in Fig. 3*B*,

TABLE 1. *Size and surface charge of different NP formulations*

NP formulation	% loading (w/w)	Entrapment efficiency (%)	Size (nm)[a]	Charge (mV)[b]
Dexamethasone NP	5	28.8	98 ± 6	−5.26 ± 0.3
DNA NP	2.1	89.8	97 ± 3	−23.0 ± 1.0
Control NP	—	—	69 ± 4	−12.5 ± 0.4

[a] Mean size of NPs (±SE) counted from 10 different TEM fields.
[b] Mean zeta potential (±SE, *n* = 5) measured in 0.001 M HEPES buffer (pH 7.0).

NPs were colocalized with LysoTracker Red in the endo-lysosomal compartment within 2 min of incubation, as evident from the appearance of orange to yellow fluorescence. At 10 min postincubation, NPs were localized in the cytoplasmic compartment, as seen from the appearance of green fluorescence of NPs (Fig. 3*C*). The intensity of green fluorescence in cytoplasm increased with incubation time, which suggests the localization of more NPs in the cytoplasmic compartment with time (Fig. 3*D, E*). The above results thus indicate that NPs were probably escaping rapidly from the endo-lysosomal compartments into the cytoplasmic compartment following their uptake. This argument is supported by the fact that the brefeldin A-induced tubulation of secondary endosomes or lysosomes (20) resulted in the lack of NP-associated green fluorescence in the cytoplasmic compartment. This result may be due to the inhibition of escape of NPs from the endo-lysosomal compartment to the cytoplasmic compartment because of the tubulation of endo-lysosomal vesicles (**Fig. 4**). The above-mentioned events related to NP uptake and their cellular trafficking were then followed by using TEM. The osmium tetroxide-loaded NPs in the cells were clearly distinguishable from the intracellular vesicles because of their electron-dense nature. The TEM of the cells exposed to NPs demonstrated localization of NPs in vesicles (Fig. 3*F*) and multivesicular bodies at 10 min postincubation, with few NPs in the cytoplasm. NPs were seen adhering to the wall of endocytic vesicles, which suggests some interaction between NPs and the membrane of the endocytic vesicles prior to the escape of the NPs into the cytoplasm (Fig. 3*G*). With a further increase in the incubation time, more NPs were seen in the cytoplasmic compartment and in lysosome-like structures (Fig. 3*H*). Thus, the TEM data complement the confocal data on NP uptake and their rapid escape from the endo-lysosomal compartment to the cytoplasmic compartment.
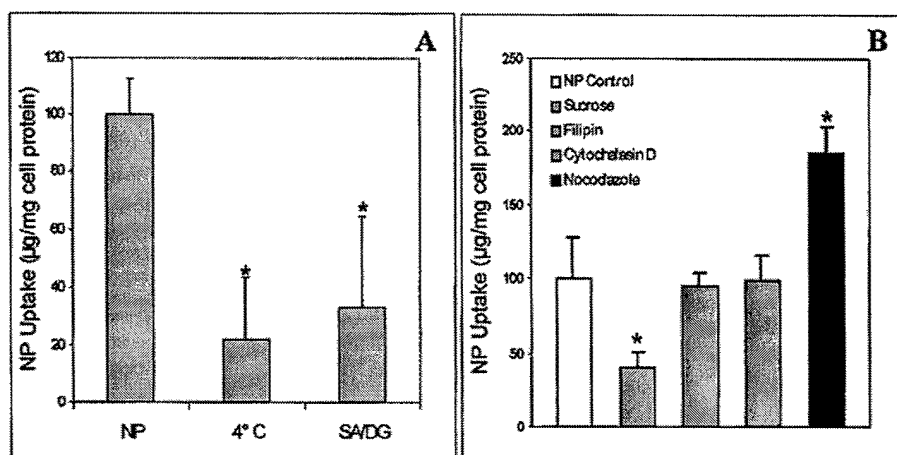
To determine the mechanism of NP escape from the endo-lysosomal compartment, we thought of various

Figure 2. Energy-dependent NP uptake by HASMCs (*A*). SA, sodium azide; DG, 6-deoxyglucose. Effect of different inhibitory agents on NP uptake in HASMCs (*B*). *$P < 0.05$.

possibilities including the changes in the surface characteristics of NPs after their cellular uptake. We found that PLGA NPs have a negative charge in physiological and alkaline pH but acquire a positive charge in the acidic pH that is present in the endo-lysosomal vesicles (pH ~4) (Fig. 1*B*). Therefore, we considered the possibility that NPs may escape the endosomes by a mechanism similar to that operating for cationic lipids. To test this hypothesis, we incubated NPs in the presence of ammonium chloride, a lysosomotropic agent that is known to raise the pH inside the endosomal vesicles. This resulted in the complete escape of the NPs from the endo-lysosomes (Fig. 4*A*). Incubation of NPs in the presence of bafilomycin A_1 also led to similar results (data not shown), probably also related to the lysosomotropic effect of bafilomycin A_1 (21). Although these results show that increasing the pH of the endo-lysosomes led to an increase in the number of NPs escaping into the cytoplasm, they did not elucidate the mechanism of escape of NPs into the cytoplasmic compartment in the absence of a lysosomotropic agent. Hence, we studied the intracellular distribution of fluorescent polystyrene NPs of similar size as PLGA NPs and without any surface functionalization. Unlike the PLGA NPs, these NPs exhibited a negative zeta potential in all pH values (Fig. 1*C*). Almost all of the polystyrene NPs were found colocalized in the endo-lysosomal compartment, with most of the cytoplasmic compartment free of the green fluorescence of NPs (Fig. 4*C*). The insignificant green fluorescence seen outside of the endo-lysosomal compartment can be attributed to the NPs localized in the early and recycling endosomes. These data support our hypothesis that surface cationization of PLGA NPs in the endo-lysosomal compartment is responsible for their escape into cytoplasm. This result is further substantiated by the fact that in the TEM pictures of the cells, PLGA NPs were clearly seen adhering to the membrane of endocytic vesicles (Fig. 3*G*) but not in the early endosomes (Fig. 3*F*), where the pH was 7 and the particles were negatively charged.

Sustained antiproliferative effect of dexamethasone-loaded NPs

The percent increase in the cell population as compared with the day 1 cell population of HA-VSMCs is shown in **Fig. 5**. Dexamethasone in solution showed inhibition of cell growth compared with plain growth medium for only up to 4 days (55 ± 2% for growth medium vs. 45 ± 4% for solution) (Fig. 5*A*). The inhibition of cell growth with dexamethasone NPs was significantly greater and more sustained (for up to 2 wk) as compared with the same dose of control NPs (Fig. 5*B*) or dexamethasone in solution (Fig. 5*C*). The inhibitory effect was not due to NPs, because there was no difference between the growth curves of the cell treated with either growth medium (Fig. 5*A*) or control NPs (Fig. 5*B*).

Sustained gene expression in prostate cancer cells

The transfection levels were dose dependent and increased with the time of transfection, which suggested sustained gene transfection with NPs (**Fig. 6**). Similar experiments with a commercially available transfecting agent, FuGene 6 (Roche Diagnostics, Indianapolis, IN), resulted in a peak expression level at 2 days, which then declined by about 70% in 3 days. The plasmid DNA in solution alone showed an insignificant level of transfection.

DISCUSSION

For macromolecular therapeutics such as plasmid DNA, peptides, or proteins, the major route of entry into the cell is by endocytosis (2). After intracellular uptake, the contents of the endocytic vesicle are delivered to lysosomes for degradation unless there are special mechanisms for the contents to escape out of the endo-lysosomes. Thus, it becomes critical in macromolecular delivery that the carrier used for intracellular delivery should also successfully protect the macro-
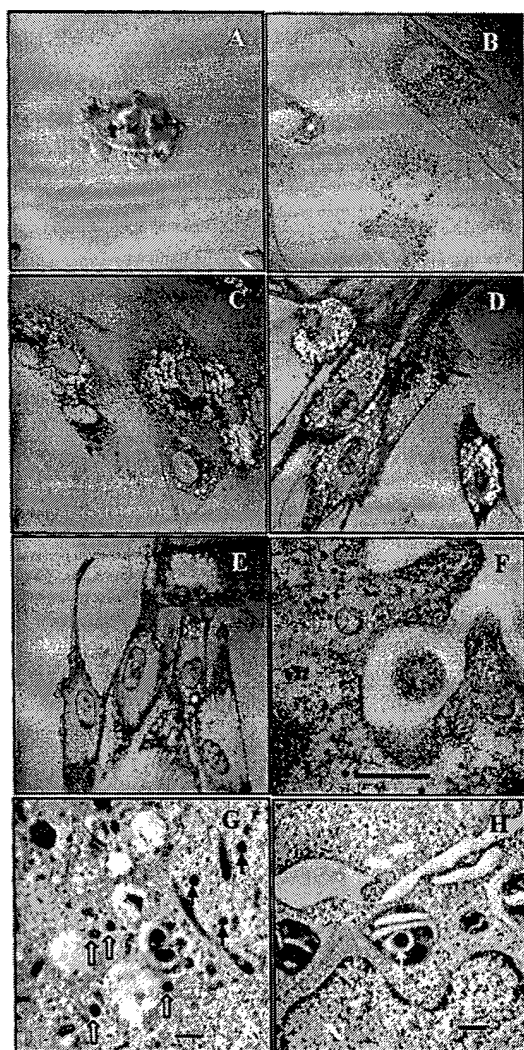
Figure 3. Colocalization of green fluorescent PLGA NPs with Texas Red transferrin (*A*, magnification 100 ×; the slight change in the cell morphology is attributed to the preincubation in serum-free medium). Rapid uptake and endo-lysosomal escape of fluorescently labeled NPs in HASMCs. Secondary endosomes and lysosomes were stained with Lyso-Tracker Red (*B* to *E*, magnification 100 ×). TEM image of NP uptake in HASMCs 10 min after NP incubation (scale bar = 100 nm) (*F*). After the uptake, NPs were found in the endocytic v esicles (*G*), with some of them appearing as interacting with the vesicle membrane and as escaping the vesicles (open arrows) and others free in the cytoplasm (arrowheads) (scale bar = 500 nm). Some NPs were also found in lysosome-like structures (white arrow in *H*) (scale bar = 500 nm). N, nucleus.

molecule from degradation in the lysosomes · and deliver it to the cytoplasmic compartment (3). Further, for drugs such as dexamethasone, receptors of which are cytoplasmic, it may be important to retain the drug in the cytoplasmic compartment to enhance its therapeutic efficacy (22).

The efficacy of NP-encapsulated therapeutic agents such as low molecular weight drugs and macromolecules has been known (10, 13, 23), but the mechanism of their enhanced therapeutic effect has not been investigated at a cellular level. Although a therapeutic agent encapsulated in NPs may be less susceptible to degradation in the endo-lysosomal compartment, the relatively faster degradation of PLGA NPs under acidic conditions in the endo-lysosomal compartment (11) may result in the release of the therapeutic agent in the endo-lysosomes, which could then degrade quite rapidly. We therefore hypothesized that to function as an efficient drug or gene delivery vehicle, NPs must be efficiently internalized into the cells and then deliver their payload into the cytoplasmic compartment rather than be retained in the degradative environment of endo-lysosomal compartment.

In our studies, PLGA NPs were internalized by VSMCs in an energy-dependent manner, which suggests an endocytic process (24). This result was further confirmed by the fact that NPs, once internalized, were found in the endosomal and lysosomal compartments. A similar energy-dependent and saturable uptake was reported for poly(ethylene oxide)-PLGA nanospheres in VSMCs, and it was suggested that the uptake was through adsorptive pinocytosis (25). NP uptake was significantly reduced after inhibition of clathrin vesicles but not caveolae. Clathrin-mediated transport has been previously reported for active receptor-mediated endocytosis (26). However, our NPs did not have any specific ligands for receptor-mediated intracellular uptake. Therefore, it is possible that NPs were being nonspecifically transported through clathrin vesicles. The fact that NPs were generally found in the center of the newly formed endocytic vesicle (Fig. 3*F*) instead of being attached to the membrane wall provides further evidence that NPs were being internalized by a nonspecific mechanism, possibly by fluid-phase pinocytosis. VSMCs are known to be phagocytic, involved in acting on dead and apoptotic cells in the vessel wall (27). However, no phagocytic cellular activity was detected during the uptake of NPs at an NP dose as high as 1000 μg (assay kit: Fc-OxyBurst, Molecular Probes). Absence of any effect on the NP uptake after the inhibition of microfilament polymerization further confirmed that the NP uptake process is not phagocytic (24).

After their uptake, NPs were localized in the early and recycling endosomes and also in the late endosomes and lysosomes. We hypothesize that from early endosomes, NPs either are recycled back to the surface or are transported to the secondary endosomes and lysosomes from which the NPs escape into the cytosol (**Fig. 7**). Similar sorting pathways at the level of early endosomes have been described for cell surface receptors that are either recycled back to the surface or degraded in the lysosomes (28). Endosomal escape has been reported for viral and nonviral vectors used in gene therapy (2, 29). Although viral vectors use a fusogen peptide to cross the endosomal membrane, it is generally believed that the DNA-cationic compound fuses with the organelle membrane, leading to the escape of DNA into the cytosol. Another possibility is that the cationic lipids and polymers cause the swelling and rupture of the lysosomes by sequestering protons

Figure 4. Mechanism of NP escape from endo-lysosomes. Increasing the pH of the endo-lysosomes with ammonium chloride resulted in the complete escape of NPs from these organelles. Arrows indicate endo-lysosomes without any NPs inside them (absence of green fluorescence) (*A*). Incubation of HASMCs with brefeldin A resulted in tubulation of secondary endosomes and lysosomes (arrows) and prevented the escape of NPs into cytoplasm (*B*). Polystyrene NPs were found mostly associated with endo-lysosomes and not in the cytoplasm (*C*). N, nucleus. Magnification 100 ×.

and their counterions (the "proton sponge effect") and create an osmotic imbalance similar to that created by lysosomotropic compounds (30). This latter mechanism could be the source of toxicity observed with the cationic vectors.

Although cationization of poly(lactide) or PLGA microparticles with the change of pH was previously reported and was attributed to the transfer of excess protons from the bulk liquid to the NP surface or attributed to hydrogen bonding between carboxyl groups of poly(lactide) or PLGA and hydronium molecules in the acidic pH (31, 32), its significance in the escape of NPs from the endo-lysosomal compartment was not elucidated. This surface cationization could explain the differences in NP behavior in the different endocytic vesicles. The early endocytic vesicles have a physiological pH (24) and at this pH, NPs would have a net negative charge and hence would be repelled by the negatively charged endosomal membrane. The

TEM of the cells exposed to NPs showed NPs in the center of the early endosomes (Fig. 3*F*), supporting the above argument. However, the secondary endosomes and lysosomes are predominantly acidic, with pH values ranging from 4 to 5 (24). In this pH, NPs would have a net cationic potential and hence would interact with the negatively charged membrane (Fig. 3*G*), leading to their escape into cytoplasmic compartment. The escape of NPs is not due to the opening of the endo-lysosomal vesicles because no differences in the distribution of LysoTracker dye was found in the cells that were incubated with NPs for 24 h (data not shown). Lysosomotropic agents are known to cause the destabilization of endo-lysosomes because of the change in the pH of the endo-lysosomal vesicles, leading to the escape of their contents (21). Because of the release of the endosomal contents, lysosomotropic agents are known to have cytotoxic effects. Because we did not observe cellular toxicity with PLGA NPs in cell culture in a 48-h
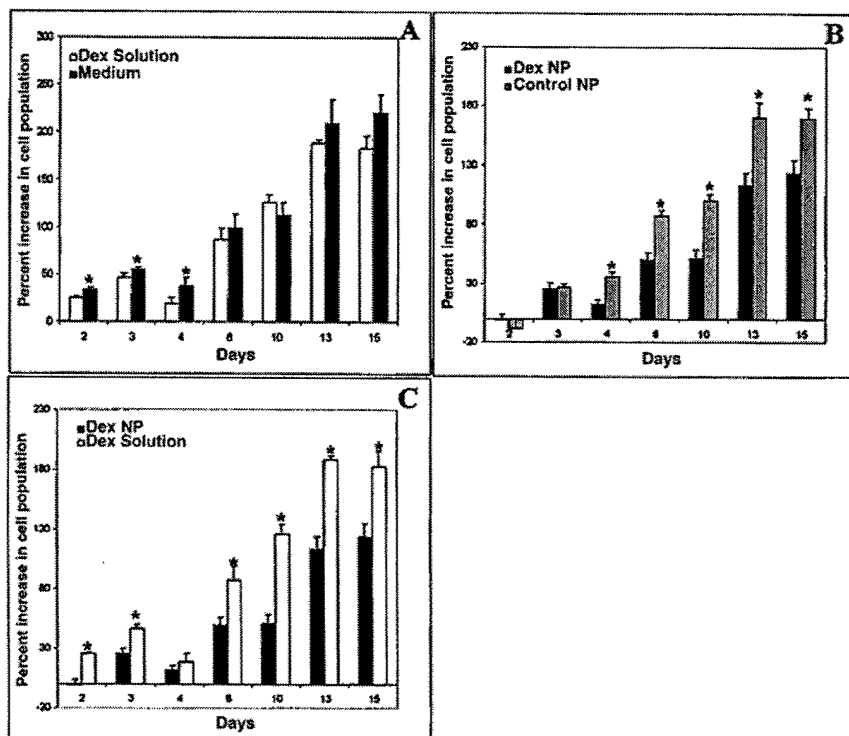
Figure 5. Sustained antiproliferative effect of dexamethasone NPs. Dexamethasone (DEX) solution showed a transient inhibition of cell proliferation compared with plain medium (*A*), although dexamethasone NPs showed a sustained and significantly greater inhibition of proliferation compared with control NPs (*B*) and with dexamethasone in solution (*C*). *$P < 0.05$. The slight reduction in cell density at day 4 could be due to detachment of few cells as a result of a medium change and washing of cells.
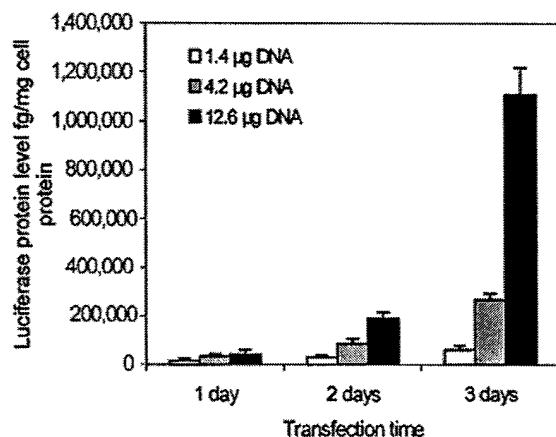
Figure 6. Sustained gene expression with DNA-loaded PLGA NPs in the PC3 cell line. Doses are presented as the amount of DNA equivalent in μg/well. Plasmid DNA alone showed negligible gene transfection (e.g., 27 ± 27 fg/mg of cell protein at 3 days for a dose of 16.2 μg of DNA/well).

mitogenic assay in our previous studies (16), it is clear that NPs do not open up the endo-lysosomal vesicles and are probably released by localized destabilization of the endo-lysosomal membrane at the point of contact with NP, followed by extrusion of the NP through the membrane (Fig. 3G). This hypothesis of NP escape from the endosomal compartment was further confirmed by the fact that polystyrene NPs, which did not show a charge reversal in the acidic pH as did PLGA NPs, were retained in the early and recycling endosomes or in the secondary endosomes, with most of the cytoplasmic compartment free of NP-associated green fluorescence (Fig. 4C).

This mechanism of action of NPs is an important advantage in the use of PLGA NPs as cytoplasmic delivery vehicles. Unlike cationic lipids or polymers, PLGA NPs are cationic only in the endosomal compartment and do not destabilize the lysosomes. This reduces the chances of toxicity commonly associated with the use of cationic lipids and cationic polymers (33). Further, the intracellular uptake of the NPs is unaffected by serum (unpublished observation) and hence PLGA NPs are suitable for in vivo applications. NPs retained intracellularly could release the encapsulated drug slowly, leading to a sustained drug effect, which is especially crucial for drugs that require intracellular uptake. As a proof of this concept, we demonstrated a sustained and significantly greater antiproliferative efficacy of NP-encapsulated dexamethasone compared with dexamethasone in solution. Dexamethasone in solution showed inhibition while the cells were in contact with the drug (4 days). After the drug was removed (growth medium containing dexamethasone was replaced with fresh growth medium without any drug), the inhibitory effect of the drug was lost (Fig. 5A). However, with NPs, a proportion of NPs would have entered the cytoplasm and remained there, slowly releasing the drug. This particular formulation of dexamethasone showed an approximate 70% drug release

during 7 days under in vitro sink conditions (data not shown). Thus, despite removing NPs from the medium, cells would still have a continuous supply of the drug because of the NPs localized intracellularly. This result is reflected in the antiproliferative efficacy: the inhibition of cell proliferation in the dexamethasone NP group was significantly greater and sustained compared with the dexamethasone solution group (Fig. 5C). Intracellular sustained release of the drug coupled with the fact that the receptors for dexamethasone are cytoplasmic could have resulted in the observed enhancement of NP-encapsulated dexamethasone. Results of these studies could explain the significant decrease in neointimal formation observed in our previous studies with localized delivery of dexamethasone-loaded NPs compared with the controls in a rat carotid model of restenosis (13).

In addition, we hypothesized that for NPs to function as a gene transfection system they should escape the endo-lysosomal compartment and slowly release the encapsulated DNA in the cytosol, resulting in sustained gene expression. To demonstrate this concept, we showed sustained gene expression of a marker gene in a prostate cancer cell line. The sustained gene expression observed in this study further substantiates the fact that NPs escape the endo-lysosomal compartment and that the DNA from the NPs is released slowly in the cytoplasmic compartment for their nuclear localization. We previously showed that encapsulated plasmid
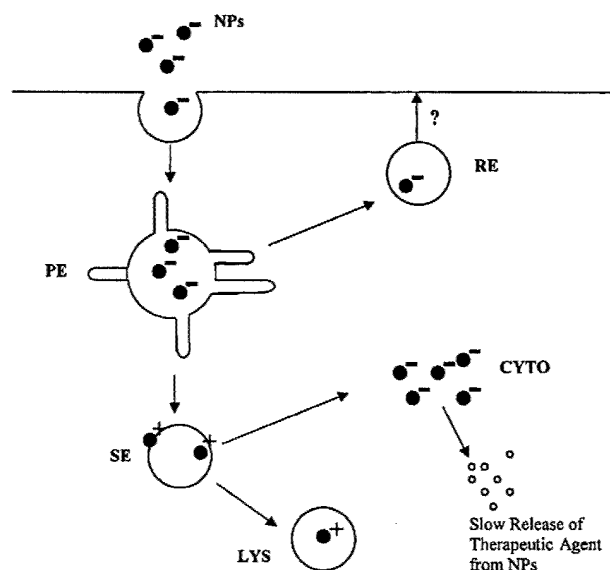
Figure 7. Schematic depicting the intracellular uptake and endo-lysosomal escape of PLGA NPs. After their internalization by nonspecific fluid phase endocytosis, NPs (depicted as closed circles) are transported to early or primary endosomes (PE), from which they could be sorted to either recycling endosomes (RE) or secondary endosomes (SE). In the acidic pH of the secondary endosomes, the surface charge of NPs changes from anionic to cationic, resulting in a local NP-membrane interaction leading to the escape of NPs into the cytoplasm (CYTO). A fraction of NPs is also transported to lysosomes (LYS).

DNA is released at a sustained rate from PLGA nanoparticles (82% cumulative release during 17 days) under in vitro sink conditions (12). Transfection experiments with a commercially available transfecting agent, FuGene 6 (6:1 FuGene 6:DNA, 0.2 μg of DNA/well, Roche Diagnostics), resulted in a peak expression level at 2 days (250,000 pg/mg of cell protein), which then declined by about 70% in 3 days, suggesting that sustained gene expression observed with NPs could be due to the sustained intracellular release of DNA from NPs.

CONCLUSIONS

We demonstrated here the rapid endo-lysosomal escape of a polymeric nanoparticulate carrier formulated from PLGA. The endo-lysosomal escape of these NPs occurs because of their selective surface charge reversal in the acidic endo-lysosomes. After their escape, NPs deliver their payload in the cytoplasm at a slow rate, leading to a sustained therapeutic effect. Because NPs are biodegradable and biocompatible and are capable of sustained intracellular delivery of multiple classes of cargoes, they are a suitable system for intracytoplasmic delivery of drugs, proteins, or genes. 𝔽𝕁

REFERENCES

1. Riezman, H., Woodman, P. G., van Meer, G., and Marsh, M. (1997) Molecular mechanisms of endocytosis. *Cell* **91**, 731–738
2. Wattiaux, R., Laurent, N., Conninck, S. W., and Jadot, M. (2000) Endosomes, lysosomes: their implication in gene transfer. *Adv. Drug Deliv. Rev.* **41**, 201–208
3. Tachibana, R., Harashima, H., Shono, M., Azumano, M., Niwa, M., Futaki, S., and Kiwada, H. (1998) Intracellular regulation of macromolecules using pH-sensitive liposomes and nuclear localization signal: qualitative and quantitative evaluation of intracellular trafficking. *Biochem. Biophys. Res. Commun.* **251**, 538–544
4. Torchilin, V. P., Rammohan, R., Weissig, V., and Levchenko, T. S. (2001) TAT peptide on the surface of liposomes affords their efficient intracellular delivery even at low temperature and in the presence of metabolic inhibitors. *Proc. Natl. Acad. Sci. USA* **98**, 8786–8791
5. Cotten, M., Wagner, E., Zatloukal, K., Phillips, S., Curiel, D. T., and Birnstiel, M. L. (1992) High-efficiency receptor-mediated delivery of small and large 48 kilobase gene constructs using the endosome-disruption activity of defective or chemically inactivated adenovirus particles. *Proc. Natl. Acad. Sci. USA* **89**, 6094–6098
6. Maheshwari, A., Mahato, R. I., McGregor, J., Han, S., Samlowski, W. E., Park, J. S., and Kim, S. W. (2000) Soluble biodegradable polymer-based cytokine gene delivery for cancer treatment. *Mol. Ther.* **2**, 121–130
7. Lindgren, M., Hallbrink, M., Prochiantz, A., and Langel, U. (2000) Cell-penetrating peptides. *Trends Pharmacol. Sci.* **21**, 99–103
8. Morris, M. C., Depollier, J., Mery, J., Heitz, F., and Divita, G. (2001) A peptide carrier for the biologically active proteins into mammalian cells. *Nat. Biotechnol.* **19**, 1173–1176
9. Schwarze, S. R., and Dowdy, S. F. (2000) In vivo protein transduction: intracellular delivery of biologically active proteins, compounds and DNA. *Trends Pharmacol. Sci.* **21**, 45–48
10. Labhasetwar, V. (1997) Nanoparticles for drug delivery. *Pharm. News* **4**, 28–31
11. Shive, M. S., and Anderson, J. M. (1997) Biodegradation and biocompatibility of PLA and PLGA microspheres. *Adv. Drug Deliv. Rev.* **28**, 5–24
12. Labhasetwar, V., Bonadio, J., Goldstein, S. A., and Levy, R. J. (1999) Gene transfection using biodegradable nanospheres: results in tissue culture and a rat osteotomy model. *Colloids Surfaces B Biointerfaces* **16**, 281–290
13. Guzman, L. A., Labhasetwar, V., Song, C., Jang, Y., Lincoff, A. M., Levy, R., and Topol, E. J. (1996) Local intraluminal infusion of biodegradable polymeric nanoparticles. A novel approach for prolonged drug delivery after balloon angioplasty. *Circulation* **94**, 1441–1448
14. Cohen, H., Levy, R. J., Gao, J., Fishbein, I., Kousaev, V., Sosnoski, S., Slomkowski, S., and Golomb, G. (2000) Sustained delivery and expression of DNA encapsulated in polymeric nanoparticles. *Gene Ther.* **7**, 1896–1905
15. Langer, R. (1997) Tissue engineering: a new field and its challenges. *Pharm. Res.* **14**, 840–841
16. Davda, J., and Labhasetwar, V. (2002) Characterization of nanoparticle uptake by endothelial cells. *Int. J. Pharm.* **233**, 51–59
17. Belannger, A. J., Scaria, A., Lu, H., Sullivan, J. A., Cheng, S. H., Gregory, R. J., and Jiang, C. (2001) Fas ligand/Fas-mediated apoptosis in human artery smooth muscle cells: therapeutic implications of fratricidal mode of action. *Cardiovasc. Res.* **51**, 749–761
18. Panyam, J., Lof, J., O'Leary, E., and Labhasetwar, V. (2002) Efficiency of Dispatch® and Infiltrator® cardiac infusion catheters in arterial localization of nanoparticles in a porcine coronary model of restenosis. *J. Drug Target.* In press
19. Peters, P. J., Gao, M., Gaschet, J., Ambach, A., van Donselaar, E., Traverse, J. F., Bos, E., Wolffe, E. J., and Hsu, V. W. (2001) Characterization of coated vesicles that participate in endocytic recycling. *Traffic* **2**, 885–895
20. Wagner, M., Rajasekaran, A. K., Hanzel, D. K., Mayor, S., and Rodriguez-Boulan, E. (1994) Brefeldin A causes structural and functional alterations of the trans-Golgi network of MDCK cells. *J. Cell Sci.* **107**, 933–943
21. Shitara, Y., Kato, Y., and Sugiyama, Y. (1998) Effect of brefeldin A and lysosomotropic reagents on the intracellular trafficking of epidermal growth factor and transferrin in Madin-Darby canine kidney epithelial cells. *J. Control. Release* **55**, 35–43
22. Adcock, I. M. (2000) Molecular mechanisms of glucocorticosteroid actions. *Pulm. Pharmacol. Ther.* **13**, 115–126
23. Moghimi, S. M., Hunter, A. C., and Murray, J. C. (2001) Long-circulating and target specific nanoparticles: theory to practice. *Pharmacol. Rev.* **53**, 283–318
24. Mukherjee, S., Ghosh, R. N., and Maxfield, F. R. (1997) Endocytosis. *Physiol. Rev.* **77**, 759–803
25. Suh, H., Jeong, B., Liu, F., and Kim, S. W. (1998) Cellular uptake study of biodegradable nanoparticles in vascular smooth muscle cells. *Pharm. Res.* **15**, 1495–1498
26. Gicquiaux, H., Lecat, S., Gaire, M., Dieterlen, A., Mely, Y., Takeda, K., Bucher, B., and Galzi, J. (2002) Rapid internalization and recycling of the human neuropeptide Y Y_1 receptor. *J. Biol. Chem.* **277**, 6645–6655
27. Bennet, M. R., Gibson, D. F., Schwartz, S. M., and Tait, J. F. (1995) Binding and phagocytosis of apoptotic vascular smooth muscle cells is mediated in part by exposure of phosphatidylserine. *Circ. Res.* **77**, 1136–1142
28. Gruenberg, J. (2001) The endocytic pathway: a mosaic of domains. *Nat. Rev. Mol. Cell. Biol.* **2**, 721–730

29. Liu, F., and Huang, L. (2002) Development of non-viral vectors for systemic gene delivery. *J. Control. Release* **78,** 259–262

30. Boussif, O., Lezoualc'h, F., Zanta, M. A., Mergny, M. D., Scherman, D., Demeneix, B., and Behr, J. P. (1995) A versatile vector for gene and oligonucleotide transfer into cells in culture and in vivo: polyethylenimine. *Proc. Natl. Acad. Sci. USA* **92,** 7297–7301

31. Stolnik, S., Garnett, M. C., Davies, M. C., Illum, L., Bousta, M., Vert, M., and Davis, S. S. (1995) The colloidal properties of surfactant-free biodegradable nanospheres from poly(β-malic acid-*co*-benzyl malate)s and poly(lactic acid-*co*-glycolide). *Colloids Surfaces A Physicochem. Eng. Aspects* **97,** 235–245

32. Makino, K., Ohshima, H., and Kondo, T. (1986) Transfer of protons from bulk solution to the surface of poly(L-lactide) microcapsules. *J. Microencapsul.* **3,** 195–202

33. Clark, P. R., and Hersh, E. M. (1999) Cationic lipid-mediated gene transfer: current concepts. *Curr. Opin. Mol. Ther.* **1,** 158–176

ELSEVIER

Residual polyvinyl alcohol associated with poly (D,L-lactide-co-glycolide) nanoparticles affects their physical properties and cellular uptake

Sanjeeb K. Sahoo[a], Jayanth Panyam[a], Swayam Prabha[a], Vinod Labhasetwar[a,b,*]

[a]*Department of Pharmaceutical Sciences, University of Nebraska Medical Center 986025, Omaha, NE 68198-6025, USA*
[b]*Department of Biochemistry and Molecular Biology, University of Nebraska Medical Center 986025, Omaha, NE 68198, USA*

Abstract

Polyvinyl alcohol (PVA) is the most commonly used emulsifier in the formulation of poly lactide and poly (D,L-lactide-co-glycolide) (PLGA) polymeric nanoparticles. A fraction of PVA remains associated with the nanoparticles despite repeated washing because PVA forms an interconnected network with the polymer at the interface. The objective of this study was to determine the parameters that influence the amount of residual PVA associated with PLGA nanoparticles and its effect on the physical properties and cellular uptake of nanoparticles. Nanoparticles were formulated by a multiple emulsion-solvent evaporation technique using bovine serum albumin (BSA) as a model protein. The parameters that affected the amount of residual PVA include the concentration of PVA and the type of organic solvent used in the emulsion. The residual PVA, in turn, influenced different pharmaceutical properties of nanoparticles such as particle size, zeta potential, polydispersity index, surface hydrophobicity, protein loading and also slightly influenced the in vitro release of the encapsulated protein. Importantly, nanoparticles with higher amount of residual PVA had relatively lower cellular uptake despite their smaller particle size. It is proposed that the lower intracellular uptake of nanoparticles with higher amount of residual PVA could be related to the higher hydrophilicity of the nanoparticle surface. In conclusion, the residual PVA associated with nanoparticles is an important formulation parameter that can be used to modulate the pharmaceutical properties of PLGA nanoparticles. © 2002 Elsevier Science B.V. All rights reserved.

Keywords: Polyvinyl alcohol; Particle size; Sustained release; Intracellular uptake; Hydrophobicity

1. Introduction

There is an increased interest in developing biodegradable nanoparticles since they offer a suitable means of delivering small molecular weight drugs, proteins or genes by either localized or targeted delivery to the tissue of interest [1]. Nanoparticles are colloidal systems that range in size typically from 10 to 1000 nm in diameter, and are formulated from a biodegradable polymer in which the therapeutic agent is entrapped in, adsorbed or chemically coupled onto the polymer matrix [2]. Although a number of different polymers have been investigated for formulating biodegradable nanoparticles, poly (D,L-

*Corresponding author. Tel.: +1-402-559-9021; fax: +1-402-559-9543.

E-mail address: vlabhase@unmc.edu (V. Labhasetwar).

lactide-co-glycolide) (PLGA) and poly lactic acid (PLA), FDA approved biocompatible and biodegradable polymers, have been the most extensively studied [3,4]. Emulsion-solvent evaporation is the commonly used method to formulate PLA and PLGA nanoparticles and poly (vinyl alcohol) (PVA) is the emulsifier most commonly used to stabilize the emulsion since it forms particles of relatively small size and uniform size distribution [5,6]. A fraction of PVA remains associated with the nanoparticles despite repeated washing because PVA forms an interconnected network with the polymer at the interface [7]. Since the residual PVA associated with the surface of nanoparticles could be up to 13% w/w of nanoparticles [6], we hypothesized that it could influence the different physical properties of nanoparticles and their interactions with the surrounding environment including with that of the cell membrane. The overall goal of the study, therefore, was to determine the effect of residual PVA associated with nanoparticles on their physical and intracellular uptake properties.

2. Methods

2.1. Materials

PLGA (MW 143 900 Da, copolymer ratio 50:50) was purchased from Birmingham Polymers, Inc. (Birmingham, AL). Polyvinyl alcohol (PVA, average MW 30 000–70 000 Da), Bovine serum albumin (Fraction V) and Rose Bengal were purchased from Sigma (St. Louis, MO). 6-coumarin was obtained from Polysciences Inc. (Warrington, PA).

2.2. Nanoparticle formulation

Nanoparticles were formulated using a multiple emulsion-solvent evaporation technique as per the previously published protocol [8]. In brief, an aqueous solution of BSA (300 μl, 10% w/v) was emulsified in an organic phase consisting of 90 mg PLGA and 50 μg of 6-coumarin dissolved in 3 ml of chloroform to form a primary oil-in-water emulsion. The above emulsion was further emulsified in an aqueous PVA solution (12 ml, concentration of PVA was varied from 0.5 to 5% w/v depending upon the

protocol) to form a multiple water-in-oil-in-water emulsion. The emulsification was carried out using a microtip probe sonicator set at 55 W of energy output (XL 2015 Sonicator® ultrasonic processor, Misonix Inc., Farmingdale, NY) for 2 min over an ice-bath. The emulsion was stirred overnight on a magnetic stir plate to allow the evaporation of chloroform. Nanoparticles were recovered by ultracentrifugation at 110 000×g for 20 min at 4 °C (Beckman Optima™ LE-80K, Beckman Instruments, Inc., Palo Alto, CA), washed twice with water to remove PVA and then lyophilized for 2 days (VirTis Company, Gardiner, NY). The fluorescent 6-coumarin dye incorporated in nanoparticles serves as a good marker for nanoparticles as the dye does not leach from the nanoparticles, and has been used in our previous studies to determine the cellular and tissue uptake of nanoparticles [8,9]. To study the effect of different organic solvents used to dissolve the polymer on the nanoparticle properties, an identical protocol was used except that the chloroform was replaced with the respective organic solvent (acetone or dichloromethane) and the PVA concentration was kept at 5% w/w in the aqueous phase for all the formulations.

2.3. Particle size analysis and zeta potential

Particle size and size distribution was determined by photon correlation spectroscopy (PCS) using quasi-elastic light scattering equipment. A dilute suspension of nanoparticles (100 μg/ml) was prepared in double distilled water and sonicated on an ice bath for 30 s. The sample was subjected to particle size analysis in the ZetaPlus™ particle size analyzer (Brookhaven Instrument Corp, Holtsville, NY). To measure zeta potential of nanoparticles as a function of pH, a suspension of nanoparticles was prepared as above in 0.001 M HEPES buffer of different pH (pH adjusted either with 0.1 M HCl or 0.1 M NaOH). The zeta potential was measured immediately using the ZetaPlus™ zeta potential analyzer.

2.4. Determination of residual PVA

The amount of PVA associated with nanoparticles was determined by a colorimetric method based on

the formation of a colored complex between two adjacent hydroxyl groups of PVA and an iodine molecule [10]. Briefly, 2 mg of lyophilized nanoparticle sample was treated with 2 ml of 0.5 M NaOH for 15 min at 60 °C. Each sample was neutralized with 900 µl of 1 N HCl and the volume was adjusted to 5 ml with distilled water. To each sample, 3 ml of a 0.65 M solution of boric acid, 0.5 ml of a solution of I_2/KI (0.05 M/0.15 M), and 1.5 ml of distilled water were added. Finally, the absorbance of the samples was measured at 690 nm after 15 min incubation. A standard plot of PVA was prepared under identical conditions.

2.5. Hydrophobicity of nanoparticles

The binding constant of Rose Bengal to the surface of the nanoparticles was used as the measure of surface hydrophobicity [11]. A sample of various formulations of nanoparticles (1 mg) was incubated with different concentrations (5–40 µg/ml) of Rose Bengal dye for 3 h at room temperature. The samples were centrifuged at 14 000 rev./min for 30 min in a microcentrifuge (Eppendorf 5417R, Brinkmann Instruments, Westbury, NY) to spin down the particles. The supernatant from each sample was analyzed spectrophotometrically at 542.7 nm to determine the unbound dye. The dye solution without nanoparticles as a control was run each time under similar conditions to account for the dye that might bind to the centrifuge tubes. The binding constant was calculated using a Scatchard plot according to the equation:

$$r/a = KN - Kr$$

where r is the amount of Rose Bengal adsorbed per mg nanoparticles (µg/mg); a is equilibrium concentration of Rose Bengal (µg/ml); K is the binding constant (ml/µg); and N is the maximum amount bound (µg/mg).

2.6. Determination of protein loading

Protein loading in the nanoparticles was determined by analyzing the washings from the nanoparticle formulation for the protein that is not encapsulated. Protein content was measured by BCA protein assay kit (Pierce, Rockford, IL). The amount of

protein encapsulated in the nanoparticles was determined from the total amount of protein added and the amount of protein that was not encapsulated.

2.7. In vitro BSA release from nanoparticles

Release of BSA from the nanoparticles formulated using either 0.5 or 5% PVA as emulsifier was determined in phosphate buffer saline (PBS, 0.15 M, pH 7.4) at 37 °C utilizing double chamber diffusion cells placed on a shaker at 100 rev./min (Environ® orbital shaker, Lab Line, Melrose Park, IL). The donor chamber was filled with 2.5 ml of nanoparticle suspension (2.5 mg/ml) and the receiver end was filled with buffer. A Millipore® hydrophilic low protein binding membrane (Millipore Co., Bedford, MA) with 0.1 µm pore size was placed between the two chambers. The protein is freely permeable across the membrane. At predetermined intervals, the receiver chamber fluid was replaced with fresh buffer and the BSA content was analyzed using BCA protein assay.

2.8. Intracellular nanoparticle uptake

Human arterial smooth muscle cells (HASMC, Cascade Biologics, Portland, OR) were used for investigating the cellular uptake of nanoparticles. HASMCs were maintained on Medium 231 supplemented with smooth muscle growth supplement (Cascade Biologics). For nanoparticle uptake study, 24-well plates were seeded with cells at 50 000 per well density and the cells were allowed to attach for 24 h. The medium in each well was replaced with 1 ml of freshly prepared nanoparticle suspension in the medium (100 or 200 µg/well) and the plates were incubated for 1 h. The cells were then washed three times with PBS to remove the nanoparticles which were not internalized. The cells were then lysed by incubating them with 0.1 ml of 1× cell culture lysis reagent (Promega, Madison, WI) for 30 min at 37 °C. A 5 µl of each cell lysate aliquot was used for the cell protein determination and the remaining portion was lyophilized. The dye from the nanoparticles in the lyophilized samples was extracted by shaking each sample with 1 ml methanol at 37 °C for 48 h at 150 rev./min using an Environ® orbital shaker. The samples were centrifuged at 14 000 rev./min for 10

min in a microcentrifuge to remove cell debris. The supernatant was analyzed for 6-coumarin by a high-performance liquid chromatography (HPLC) method described previously [8]. A standard plot with different concentration of nanoparticles was constructed simultaneously under similar conditions to determine the amount of nanoparticles in cell lysates. The data was normalized to per milligram cell protein.

3. Results and discussion

3.1. Factors influencing the amount of residual PVA

In the formulation of PLGA nanoparticles, a fraction of PVA that is used as the emulsifier forms a stable network on the polymer surface and can not be removed during the washing procedure [12]. Initially, we investigated the effect of various formulation factors that could influence the amount of residual PVA that stays associated with PLGA nanoparticles. These include the concentration of PVA in the external aqueous phase and the organic solvent used to make the polymer solution.

3.1.1. Influence of the organic solvent used

The polarity of organic solvent used in the emulsion formation during the nanoparticle formulation might affect the amount of PVA adsorbing at the polymer-organic solvent–water interface. Therefore, nanoparticles with three different organic solvents (acetone, dichloromethane and chloroform) were formulated under identical conditions. It was found that the residual PVA associated with the nanoparticles increased with increasing solvent miscibility

Table 1
Effect of organic solvent on %residual PVA associated with nanoparticles

Solvent	Miscibility in water (Parts)[a]	Residual PVA (%±S.E.M) (w/w) (n=3)
Acetone	Freely miscible	7.45±0.62
Dichloromethane	1 in 50	6.15±0.35
Chloroform	1 in 200	4.87±0.49

[a] Merck index.

with water (Table 1). The results can be explained on the basis that more PVA might have partitioned into the polymeric phase containing an organic solvent that is more miscible with the aqueous phase, resulting in the higher deposition of PVA on the surface of nanoparticles. The results also suggest that the composition of the co-solvent system such as the combination of chloroform and acetone that is sometimes used in the formulation could also affect the residual PVA associated with nanoparticles, and hence their pharmaceutical properties.

3.1.2. PVA concentration in the external aqueous phase

To study the influence of different PVA concentrations in the external aqueous phase on the residual PVA associated with nanoparticles, we prepared nanoparticles by using chloroform as a organic solvent and with an external aqueous phase consisting of different concentrations of PVA. As shown in Fig. 1, an increase in PVA concentration in the external aqueous phase from 0.5 to 5% w/v results in the increase in the residual PVA amount associated with nanoparticles. The mechanism of PVA binding has been proposed to be due to the interpenetration of PVA and PLGA molecules during nanoparticle formulation. The hydrophobic segments of PVA penetrate into the organic phase and remain entrapped into the polymeric matrix of the nanoparti-
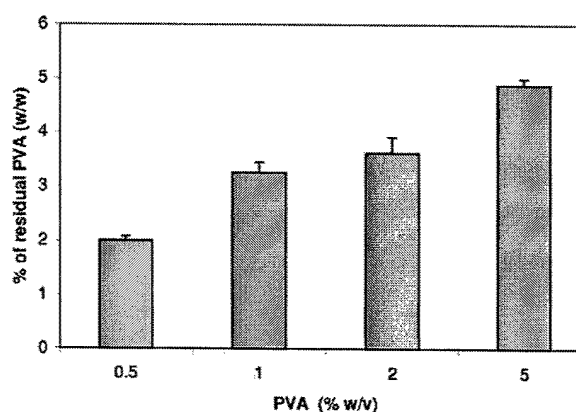

Fig. 1. Effect of PVA concentration in the external aqueous phase of the multiple emulsion used for nanoparticle formulation on the percent of residual PVA associated with nanoparticles, data as mean±S.E.M. (n=3).

cles [12]. The binding of PVA on the particle surface is likely to happen when the organic solvent is removed from the interface in which interpenetration of PVA and PLGA molecules takes place. Partially hydrolyzed PVA is a copolymer of poly(vinyl acetate) and poly (vinyl alcohol) with considerable block copolymer character. The hydrophobic vinyl acetate part serves as an anchor polymer at the oil interface for binding to the surface of PLGA polymer during the formulation. Thus, the higher PVA concentration of the continuous phase could lead to an increase in PVA molecule density at the o/w interface of the emulsion droplet, which might increase the thickness of PVA on the surface. Lee et al. demonstrated that the PVA content per weight of microparticles increases with the specific surface area as the particle size decreases [13]. They have shown that the surface PVA density (PVA content per unit surface area) of microparticles changes with the particle size in a biphasic manner. In the size range larger than 1 μm, the surface PVA density increases as the particle size decreases. However, below 1 μm, the surface density remains unchanged with the decrease in particle size.

Zambaux et al. have also reported similar increase in the amount of residual PVA with the increase in PVA concentration in external aqueous phase for PLA nanoparticles [6]. However, the amount of residual PVA associated with our PLGA nanoparticles was comparatively lower (6.15% w/w, Table 1 for dichloromethane) than that reported in the above study (13% w/w). The difference could be due to the hydrophobic nature of PLA over PLGA and/or due to the lower molecular weight of the PVA that was used in their study compared to that used in our study (13 000 to 23 000 Da vs. 30 000 to 70 000 Da).

3.2. Influence of residual PVA on pharmaceutical properties of nanoparticles

3.2.1. Size and size distribution

The mean particle size of the nanoparticles was a function of PVA concentration in the external aqueous phase (Table 2). The mean nanoparticle size decreased from 520 to 380 nm with an increase in the PVA concentration in the external aqueous phase from 0.5 to 5% w/v. A number of previous reports demonstrated that by increasing the PVA concentration in the external aqueous phase the size of the nanoparticles decreases [6,13].

This drop in the particle size with the increase in PVA concentration is probably due to the differences in the stability of the emulsions formulated with different concentrations of PVA. At concentrations lower than 2.5% w/v, PVA exists as single molecules in solution. Above this concentration, it exists in an aggregated form and has an enhanced surfactant activity. Further, the viscosity of PVA solution increases with increasing PVA concentrations (2.1 cps for 2% to 5.7 cps for 5%) (Table 2). This could result in the formation of a stable emulsion with smaller and uniform droplet size, leading to the formation of smaller sized nanoparticles with low polydispersity [6,14].

3.2.2. Zeta potential

The zeta potential values for nanoparticles pre-

Table 2
Physicochemical characteristics of the PLGA nanoparticles

PVA concentration (% w/v) used	Relative viscosity of PVA solution[a] (cps) ($n=3$)	Mean particle size (nm)[b] ($n=5$)	Polydispersity index ($n=5$)	Zeta potential S.E.M. (mV)[c] ($n=5$)	Protein loading (mg/100 mg nanoparticles)	Binding constant (K) of Rose Bengal (ml/μg) ($n=3$)
0.5	1.20	522	0.20	−15.4±0.8	19.0	0.024
1.0	1.41	468	0.20	−11.3±0.8	20.9	0.014
2.0	2.06	421	0.14	−12.5±0.4	22.3	0.013
5.0	5.70	380	0.12	−08.0±2.3	24.0	0.005

[a] Measured using Ostwald's viscometer with water as reference standard at room temperature.
[b] Mean hydrodynamic diameter measured by photon correlation spectroscopy.
[c] Measured in 0.001 M HEPES buffer, pH 7.0.

pared with different PVA concentrations are shown in Table 2. All the nanoparticles were negatively charged at pH 7, which could be attributed to the presence of ionized carboxyl groups on the surface of the nanoparticles. Fig. 2 shows the changes in the zeta potential of the nanoparticles with pH. The zeta potential–pH profiles show that the zeta potential is negative at neutral and higher pH, whilst at lower pH, there is a charge reversal and the nanoparticles acquire positive zeta potential. The above phenomenon was observed for all the formulations of nanoparticles prepared using different concentrations of PVA. However, the zeta potential values were higher for nanoparticles prepared with 0.5% PVA compared to those prepared with 5% PVA at both lower and higher pH values.

It has been reported that the zeta potential of PLGA nanoparticles without any PVA in neutral buffer is about -45 mV [15]. This high negative charge is attributed to the presence of uncapped end carboxyl groups of the polymer at the particle surface. In several studies, a clear differentiation in the zeta potential values of coated and non-coated nanoparticles was reported, with generally highly negative zeta potential values for non-coated nanoparticles and less negative zeta potential values

for coated nanoparticles. Coating of nanoparticles with some amphiphilic polymers normally decreases the zeta potential because the coating layers shield the surface charge and move the shear plane outwards from the particle surface [16,17]. Redhead et al. have reported a similar reduction in the zeta potential of PLGA nanoparticles after coating with amphilphilic polymers like poloxamer 407 and poloxamine 908 [18]. Thus, the PVA layer at the surface of the nanoparticles also probably shields the surface charge of PLGA. Since the amount of residual PVA is relatively lower in case of nanoparticles prepared with 0.5% PVA, less shielding and therefore higher zeta potential could be expected in these nanoparticles. The lower shielding effect of PVA also explains the higher zeta potential at lower or higher pH for the nanoparticles prepared with 0.5% PVA as compared to the nanoparticles prepared with 5% PVA because more carboxyl groups are available for ionization with lower amount of the nanoparticle associated PVA (Fig. 2).

Fig. 2 shows the zeta potentials of nanoparticles formulated with different concentrations of PVA. In acidic solutions (pH<5.0), the zeta potential of the PLGA nanoparticles becomes positive (Fig. 2). As the PVA concentration used in the formulation of nanoparticle was increased, the surface charge of nanoparticle becomes less positive in the acidic pH. The surface charge reversal can be attributed to the transfer of protons from the bulk solution to the surface of the nanoparticles [19,20]. Hydroxyl groups at the surface of nanoparticles can become $-OH_2^+$ by protonation. A similar charge reversal with the change in pH has been observed for polystyrene nanoparticles with carboxyl functional groups on the surface and was attributed to a positive charge acquired by hydrogen bonding of hydronium ions to the carboxylic group [15].
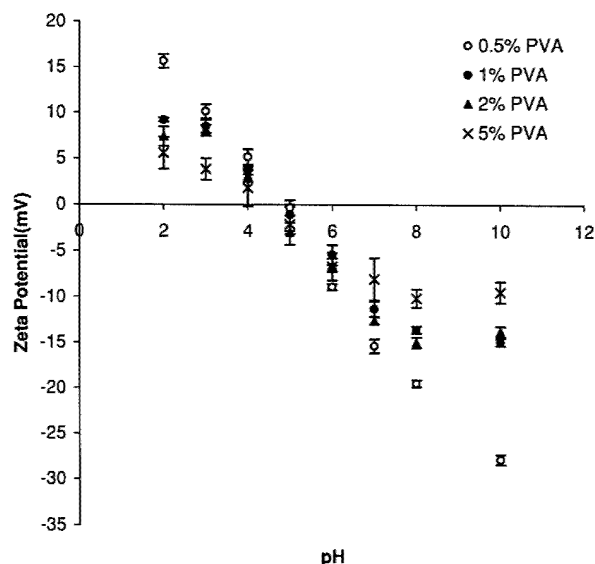
3.2.3. Surface hydrophobicity

Nanoparticles formulated with 5% PVA were found to be more hydrophilic compared to those formulated with 0.5% PVA as seen from the lower binding constants of Rose Bengal to the surface of the nanoparticles (Table 2). PVA is a hydrophilic polymer than PLGA and therefore the higher amount of residual PVA at the surface of the nanoparticles formulated with 5% PVA (Fig. 1) could account for

Fig. 2. Effect of pH on the zeta potential of nanoparticles formulated with 0.5, 1, 2 and 5% PVA concentration in aqueous phase, data as mean±S.E.M. ($n=5$).

their higher hydrophilicity. This effect could be compared to the effect of coating a hydrophilic polymer such as polyethylene glycol (PEG) or poloxamer on to a surface of a hydrophobic polymer resulting in higher hydrophilicity of the nanoparticle surface [18].

3.2.4. Protein loading in nanoparticles

The effect of PVA concentration in the external aqueous phase of the multiple emulsion on the protein loading in nanoparticles is shown in Table 2. Protein loading increased with increasing PVA concentration in the external aqueous phase (19% w/w for 0.5% PVA and 24% w/w for 5% PVA). This can be related to the increasing viscosity of the PVA solution with increasing concentration of PVA leading to the resistance to the outward diffusion of BSA from the internal aqueous phase and to the better stabilization of the emulsion at higher PVA concentrations [21]. Also, higher amount of PVA at the interface of organic phase and the external aqueous phase could have contributed to the higher resistance to BSA diffusion out of the polymeric phase leading to higher protein loading in nanoparticles prepared with higher amount of PVA.

3.2.5. In vitro release of BSA

The cumulative in vitro release of BSA from PLGA nanoparticles, using 0.5% and 5% PVA as an emulsifier is shown in Fig. 3. The release profiles were biphasic for both the formulations, with an
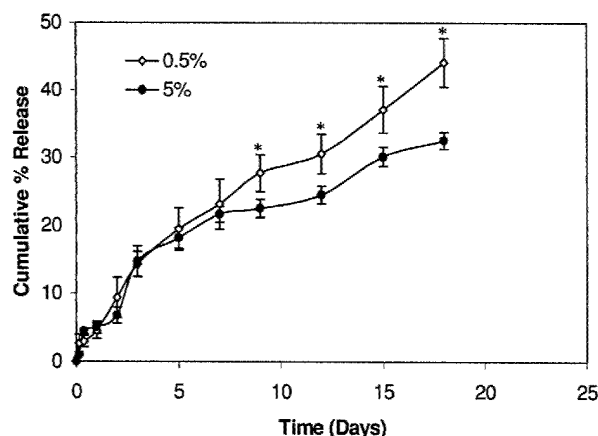
Fig. 3. Effect of residual PVA on the in vitro release of BSA from nanoparticles, data as mean±S.E.M. ($n=3$). * $P<0.05$.

initial burst release attributed to surface associated protein, followed by a slower release phase as the entrapped protein slowly diffuses out into the release medium [21]. While the residual PVA did not affect the initial release of the protein in the first 7 days, the cumulative release of the protein was slightly higher starting at 10 days for nanoparticles formulated with 0.5% PVA. The possibility is that the higher viscosity of 5% PVA solution could have resulted in a more compact polymer matrix resulting in lowered degradation rate of the polymer and/or the slower diffusion of the encapsulated protein from the nanoparticles. Classically, the protein release from PLGA matrices is described to be diffusion-mediated in the early phases and diffusion-cum-degradation mediated in the latter phases [22]. It could be argued, therefore, that the residual PVA does not affect the amount of protein associated with the surface of the nanoparticle but possibly influences the diffusion of the protein and the degradation of the polymer matrix. PVA is a swellable, hydrophilic macromolecule that has previously been shown to sustain the release of macromolecules [23]. Hence, it is possible that that the large amounts of PVA present on the surface could form a hydrogel barrier to the diffusional release of macromolecules.

3.2.6. Cellular uptake

Cellular uptake of different nanoparticle formulations in HAVSMCs is shown in Fig. 4A and B. Initial studies were carried out with nanoparticles formulated using different concentrations of PVA. There was no significant difference in the uptake of nanoparticles formulated with 0.5, 1 or 2% PVA (results not shown). However, the uptake was significantly reduced for nanoparticles formulated with 5% PVA (112.9 μg/mg of total cell protein for 2% PVA compared to 40 μg/mg of total cell protein for 5% PVA) at 100 μg/ml/well dose (Fig. 4A). This trend was observed at both the doses tested (100 and 200 μg/ml per well) and also in the presence or absence of serum. In general, nanoparticles demonstrated a dose dependent uptake at the two doses tested (Fig. 4B) and the presence or absence of serum did not affect the uptake.

Intracellular uptake of nano- and microparticles has previously been shown to depend on the size and the hydrophobicity of the carrier [24,25]. In general,
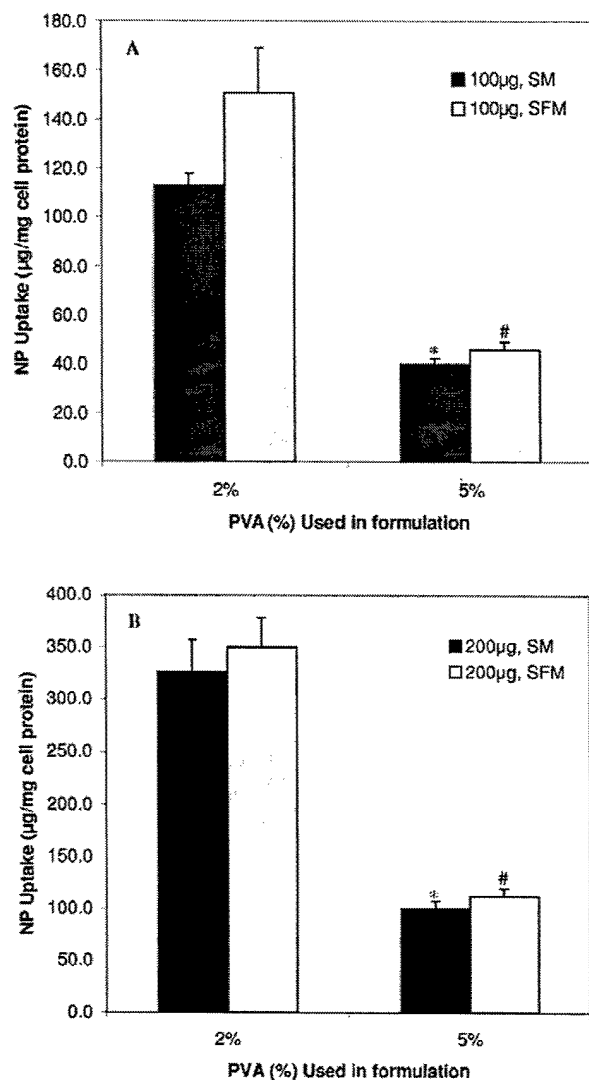
Fig. 4. Effect of residual PVA on the nanoparticle (NP) uptake in HAVSMCs. Nanoparticles were incubated with HAVSMCs at 100 μg/well (A) or 200 μg/well (B) dose in the presence or absence of serum, data as mean$\pm$S.E.M. ($n=6$). SM, serum containing medium; SFM, serum free medium; NP, nanoparticles. *,# $P<$ 0.05 compared to uptake of corresponding 2% PVA nanoparticle group.

the uptake decreases with increasing size and with increasing hydrophilicity. However, distinction has to be made in terms of the mode of intracellular uptake. Intracellular particulate uptake could either be by phagocytosis [25] or by fluid phase endocytosis [26]. A number of previous reports have demonstrated phagocytic uptake of nano- and mi-

croparticles in macrophages with a lower cut-off size for such a phagocytic uptake being about 0.5 μm [27]. For nanoparticles of lower size, the main route of intracellular entry is through fluid phase endocytosis [26]. It is also possible that the differences in the surface hydrophobicities of the two formulations (nanoparticles prepared with 5% PVA were more hydrophilic compared to those prepared with 2% PVA) could have contributed to the difference in uptake [28]. Vascular smooth cells have been reported to phagocytose other apoptotic cells and cholesterol granules in the vascular tissue [29]. However, using a phagocytosis assay kit (FcOxyBurst™, Molecular Probes, Eugene, OR), no phagocytic activity was detected even at 1000 μg/ well nanoparticle dose. Lack of any effect of serum on the nanoparticle uptake further argues against a phagocytic uptake for either of the formulation [30]. Thus, the reason for the lower uptake of nanoparticles formulated with 5% PVA despite their lower size remains unclear but appears to be related to the surface hydrophobicity of the nanoparticles.

PVA has been widely used in the formulation of biodegradable micro- and nanoparticles in different concentrations, the range being 0.5 to 10%. Traditionally, the main role of PVA has been that of an emulsion stabilizer. Previous studies by others have shown that the hydrophobic segment of PVA binds to the surface of the nanoparticles, which can not be removed during the washings [12]. Shakesheff et al. have demonstrated that PVA is adsorbed on the surface of PLA and PLGA microparticles by employing X-ray photoelectron spectroscopy [31]. While there are previous investigations that have reported the effect of PVA on the nanoparticle size and zeta potential [5,6], there is no detailed study on the effect of PVA on the cellular uptake and other pharmaceutical properties of nanoparticles. The fact that the residual PVA remains at the surface of the nanoparticles could enable it to control the way nanoparticles interact with that of a cell surface. Based on this hypothesis, we investigated the effect of residual PVA on the different pharmaceutical properties of PLGA nanoparticles. True enough, almost all of the pharmaceutical properties studied were affected by the residual PVA content. Importantly, the residual PVA significantly affected the intracellular uptake of nanoparticles.

A number of previous reports including that from our laboratory have shown the applications of biodegradable nanoparticles formulated from poly (D,L-lactide-co-glycolide) (PLGA) for drug and macromolecular delivery [32]. For a number of these applications including gene therapy, it is not only important that nanoparticles release the encapsulated therapeutic agent at a sustained rate but also release it intracellularly. Thus, efficient intracellular uptake of nanoparticles is critical for these applications. Since in our studies we have shown that the residual PVA present in the nanoparticles affects their intracellular uptake, it becomes important to consider this parameter more critically for applications that involve intracellular drug delivery. Fontana et al. have shown a significant difference between polyethylcynoacrylate nanoparticles prepared in the presence and absence of PEG and demonstrated that nanoparticles coated with PEG have reduced uptake by macrophages [33]. Further, the in vivo half-life of a carrier such as liposome or nanoparticle in the systemic circulation has been shown to depend on the surface hydrophobicity of the carrier [18]. Hydrophobic nanoparticles are rapidly cleared by circulating monocytes resulting in their localization predominantly in the liver. Gref et al. have used PEG modified block co-polymers of PLA and PLGA to formulate nanoparticles with hydrophilic properties in order to prolong their circulation time [34]. Since PVA also alters the surface hydrophobicity of nanoparticles, it would be interesting to determine if the amount of residual PVA alters the pharmacokinetics and the biodistribution of the nanoparticles in vivo.

While it is important to realize that the residual PVA influences different pharmaceutical properties of nanoparticles, it is equally important to derive strategies to control the extent the residual PVA associated with the nanoparticles. In this report, we have demonstrated that the residual PVA content can be altered by changing the PVA concentration in the external aqueous phase or by altering the type of organic solvent used in the emulsion. Further investigation is needed to study the influence of other possible parameters on the amount of residual PVA including the molecular weight and composition of the polymer, physical characteristics (hydrophilicity/hydrophobicity) of the drug incorporated in

nanoparticles, composition of co-solvents, aqueous to organic phase volume ratio of the emulsion, and the molecular weight and composition of the PVA used.

4. Conclusions

The amount of residual PVA that remains associated with the PLGA nanoparticles can be controlled by altering the PVA concentration or the type of organic solvent used in the emulsion formation, and is an important factor that influences the cellular uptake of nanoparticles. Further, the residual PVA is an important formulation parameter that can be used to modify or alter the different pharmaceutical properties of nanoparticles.

Acknowledgements

References

[1] S.M. Moghimi, A.C. Hunter, J.C. Murray, Long-circulating and target specific nanoparticles: theory to practice, Pharmacol. Rev. 53 (2) (2001) 283–318.

[2] V. Labhasetwar, Nanoparticles for drug delivery, Pharm. News 4 (1997) 28–31.

[3] R. Langer, Tissue engineering: a new field and its challenges, Pharm. Res. 14 (7) (1997) 840–841.

[4] R.A. Jain, The manufacturing techniques of various drug loaded biodegradable poly(lactide-co-glycolide) devices, Biomaterials 21 (2000) 2475–2490.

[5] P.D. Scholes, A.G.A. Coombes, L. Illum et al., The preparation of sub-200 nm poly (lactide-co-glycolide) microspheres for site-specific drug delivery, J. Controlled Release 25 (1993) 145–153.

[6] M.F. Zambaux, F. Bonneaux, R. Gref et al., Influence of experimental parameters on the characteristics of poly (lactic

acid) nanoparticles prepared by a double emulsion method, J. Controlled Release 50 (1–3) (1998) 31–40.

[7] A. Carrio, G. Schwach, J. Coudane, M. Vert, Preparation and degradation of surfactant-free PLGA microspheres, J. Controlled Release 37 (1991) 113–121.

[8] J. Davda, V. Labhasetwar, Characterization of nanoparticle uptake by endothelial cells, Int. J. Pharm. 233 (2002) 51–59.

[9] J. Panyam, J. Lof, E. O'Leary, V. Labhasetwar, Efficiency of Dispatch® and Infiltrator® cardiac infusion catheters in arterial localization of nanoparticles in a porcine coronary model of restenosis, J. Drug Target. (2002) in press.

[10] D.P. Joshi, Y.L. Lan-Chun-Fung, J.W. Pritchard, Determination of poly (vinyl alcohol) via its complex with boric acid and iodine, Anal. Chim. Acta 104 (1979) 153–160.

[11] R.H. Müller, Colloidal Carriers for Controlled Drug Delivery and Targeting, CRC Press, Boca Raton, FL, 1991.

[12] F. Boury, T. Ivanova, I. Panaiotov et al., Dynamic properties of poly (D,L-lactide) and polyvinyl alcohol monolayers at the air/water and dichloromethane air/water interfaces, J. Colloid. Interf. Sci. 169 (1995) 380–392.

[13] S.C. Lee, J.T. Oh, M.H. Jang, S.I. Chung, Quantitative analysis of polyvinyl alcohol on the surface of poly (D,L-lactide-co-glycolide) microparticles prepared by solvent evaporation method: effect of particle size and PVA concentration, J. Controlled Release 59 (2) (1999) 123–132.

[14] T. Niwa, T. Takeuchi, T. Hino, N. Kunou, Y. Kawashima, Preparation of biodegradable nanospheres of water soluble and insoluble drugs with D,L-lactide/glycolide copolymer by a novel spontaneous emulsification solvent diffusion method, and the drug release behavior, J. Controlled Release 25 (1993) 89–98.

[15] S. Stolnik, M.C. Garnett, M.C. Davies et al., The colloidal properties of surfactant-free biodegradable nanospheres from poly (β-malic acid-co-benzyl malate)s and poly (lactic acid-co-glycolide), Coll. Surf. 97 (1995) 235–245.

[16] A.E. Hawley, L. Illum, S.S. Davis, Preparation of biodegradable, surface engineered PLGA nanospheres with enhanced lymphatic drainage and lymph node uptake, Pharm. Res. 14 (5) (1997) 657–661.

[17] M. Tobio, R. Gref, A. Sanchez, R. Langer, M.J. Alonso, Stealth PLA–PEG nanoparticles as protein carriers for nasal administration, Pharm. Res. 15 (2) (1998) 270–275.

[18] H.M. Redhead, S.S. Davis, L. Illum, Drug delivery in poly (lactide-co-glycolide) nanoparticles surface modified with poloxamer 407 and poloxamine 908: in vitro characterization and in vivo evaluation, J. Controlled Release 70 (3) (2001) 353–363.

[19] K. Makino, H. Ohshima, T. Kondo, Transfer of protons from bulk solution to the surface of poly (L-lactide) microcapsules, J. Microencaps. 3 (3) (1986) 195–202.

[20] J.M. Corkill, J.F. Goodman, J. Wyer, Nuclear magnetic resonance of aqueous solutions of alkylpolyoxyethylene glycol monoethers, Trans. Faraday Soc. 65 (1969) 9–18.

[21] A.G.A. Coombes, M.-K. Yeh, E.C. Lavelle, S.S. Davis, The control of protein release from poly (DL-lactide co-glycolide) microparticles by variation of the external aqueous phase surfactant in the water-in-oil-in water method, J. Controlled Release 52 (1998) 311–320.

[22] H. Okada, One- and three-month release injectable microspheres of the LH–RH superagonist leuprorelin acetate, Adv. Drug Del. Rev. 28 (1) (1997) 43–70.

[23] V. Kushwaha, A. Bhowmick, B.K. Behera, A.R. Ray, Sustained release of antimicrobial drugs from polyvinylalcohol and gum arabica blend matrix, Artif. Cells Blood Substit. Immobil. Biotechnol. 26 (2) (1998) 159–172.

[24] M.P. Desai, V. Labhasetwar, E. Walter, R.J. Levy, G.L. Amidon, The mechanism of uptake of biodegradable microparticles in Caco-2 cells is size dependent, Pharm. Res. 14 (1997) 1568–1573.

[25] Y. Tabata, Y. Ikada, Phagocytosis of polymer microspheres by macrophages, Adv. Polymer Sci. 94 (1990) 107–141.

[26] H. Suh, B. Jeong, F. Liu, S.W. Kim, Cellular uptake study of biodegradable nanoparticles in vascular smooth muscle cells, Pharm. Res. 15 (9) (1998) 1495–1498.

[27] K.A. Foster, M. Yazdanian, K.L. Audus, Microparticulate uptake mechanisms of in-vitro cell culture models of the respiratory epithelium, J. Pharm. Pharmacol. 53 (1) (2001) 57–66.

[28] A.M. Torche, P.L. Corre, E. Albina, A. Jestin, R.L. Verge, PLGA microspheres phagocytosis by pig alveolar macrophages: influence of poly (vinyl alcohol) concentration, nature of loaded-protein and copolymer nature, J. Drug. Target. 7 (5) (2000) 343–354.

[29] M.R. Bennet, D.F. Gibson, S.M. Schwartz, J.F. Tait, Binding and phagocytosis of apoptotic vascular smooth muscle cells is mediated in part by exposure of phosphatidylserine, Circ. Res. 77 (1995) 1136–1149.

[30] J.C. Leroux, J.F. De, B. Anner, E. Doelker, R. Gurny, An investigation on the role of plasma and serum opsonins on the internalization of biodegradable poly (D,L-lactic acid) nanoparticles by human monocytes, Life Sci. 57 (7) (1995) 695–703.

[31] K.M. Shakesheff, C. Evora, I.I. Soriano, R. Langer, The adsorption of poly (vinyl alcohol) to biodegradable microparticles studied by X-ray photoelectron spectroscopy (XPS), J. Colloid. Interf. Sci. 185 (2) (1997) 538–547.

[32] J. Panyam, W.Z. Zhou, S. Prabha, S.K. Sahoo, V. Labhasetwar, Rapid endo-lysosomal escape of poly (D,L-lactide-co-glycolide) nanoparticles: implications for drug and gene delivery, FASEB J. (2002) in press.

[33] G. Fontana, M. Licciardi, S. Mansueto, D. Schillaci, G. Giammona, Amoxicillin-loaded polyethylcyanoacrylate nanoparticles: influence of PEG coating on the particle size, drug release rate and phagocytic uptake, Biomaterials 22 (21) (2001) 2857–2865.

[34] R. Gref, Y. Minamitake, M.T. Peracchia et al., Biodegradable long-circulating polymeric nanospheres, Science 263 (5153) (1994) 1600–1603.